SOCIETY FOR EXPERIMENTAL BIOLOGY

Journal of Experimental Botany, Vol. 72, No. 7 pp. 2525–2243, 2021
doi:10.1093/jxb/eraa594 Advance Access Publication 25 December 2020

RESEARCH PAPER

The cytosolic invertase NI6 affects vegetative growth, flowering, fruit set, and yield in tomato

Carla Coluccio Leskow[1], Mariana Conte[1], Talia del Pozo[2], Luisa Bermúdez[1,3], Bruno Silvestre Lira[4], Giovanna Gramegna[4], Irene Baroli[5], Estanislao Burgos[6], Diego Zavallo[1], Laura Kamenetzky[7], Ramón Asís[8], Mauricio Gonzalez[2], Alisdair Robert Fernie[9], Magdalena Rossi[4], Sonia Osorio[10,*] and Fernando Carrari,[3,6,*,†]

[1] Instituto de Biotecnología, Instituto Nacional de Tecnología Agropecuaria (IB-INTA), and Consejo Nacional de Investigaciones Científicas y Técnicas (CONICET), B1712WAA Hurlingham, Argentina
[2] Centro Tecnológico de Recursos Vegetales, Escuela de Agronomía, Universidad Mayor, Camino La Pirámide 5750, Huechuraba, Santiago, Chile
[3] Cátedra de Genética, Facultad de Agronomía, Universidad de Buenos Aires, Buenos Aires, Argentina.
[4] Departamento de Botânica, Instituto de Biociências, Universidade de São Paulo, São Paulo, SP, Brazil
[5] Instituto de Biodiversidad y Biología Experimental Aplicada., IBBEA, CONICET, Buenos Aires, Argentina
[6] Instituto de Fisiología, Biología Molecular y Neurociencias (IFIBYNE-UBA-CONICET), Ciudad Universitaria, C1428EHA Buenos Aires, Argentina
[7] Laboratorio de Genómica y Bioinformática de Patógenos. iB3 | Instituto de Biociencias, Biotecnología y Biología traslacional. Departamento de Fisiologia y Biologia Molecular y Celular Facultad de Ciencias Exactas y Naturales, Universidad de Buenos Aires, Argentina.
[8] Facultad de Ciencias Químicas, Universidad Nacional de Córdoba, Córdoba, Argentina
[9] Max Planck Institute for Molecular Plant Physiology, Wissenschafts Park Golm, Am Mühlenberg 1, Potsdam-Golm, D-14 476, Germany
[10] Instituto de Hortofruticultura Subtropical y Mediterránea "La Mayora," University of Malaga-Consejo Superior de Investigaciones Científicas, Department of Molecular Biology and Biochemistry, Campus de Teatinos, 29071 Malaga, Spain

* These authors contributed equally to this work.
† Correspondence: carrarifernando@gmail.com

Received 14 February 2020; Editorial decision 14 December 2020; Accepted 21 December 2020

Editor: Robert Hancock, The James Hutton Institute, UK

Abstract

Sucrose metabolism is important for most plants, both as the main source of carbon and via signaling mechanisms that have been proposed for this molecule. A cleaving enzyme, invertase (INV) channels sucrose into sink metabolism. Although acid soluble and insoluble invertases have been largely investigated, studies on the role of neutral invertases (A/N-INV) have lagged behind. Here, we identified a tomato *A/N-INV* encoding gene (*NI6*) co-localizing with a previously reported quantitative trait locus (QTL) largely affecting primary carbon metabolism in tomato. Of the eight *A/N-INV* genes identified in the tomato genome, *NI6* mRNA is present in all organs, but its expression was higher in sink tissues (mainly roots and fruits). A NI6-GFP fusion protein localized to the cytosol of mesophyll cells. Tomato *NI6*-silenced plants showed impaired growth phenotype, delayed flowering and a dramatic reduction in fruit set. Global gene expression and metabolite profile analyses of these plants revealed that *NI6* is not only essential for sugar metabolism, but also plays a signaling role in stress adaptation. We also identified major hubs, whose expression

patterns were greatly affected by *NI6* silencing; these hubs were within the signaling cascade that coordinates carbohydrate metabolism with growth and development in tomato.

Keywords: Carbon partitioning, cytosolic invertase, signaling, sucrose metabolism, tomato.

Introduction

The coordinated regulation of source-sink relationships is essential for normal plant growth and development. The production and distribution of plant biomass is limited by the capacity of carbon fixation and by the regulation of assimilate partitioning. Sugars are not only respiratory substrates, but also act as signal molecules in plant development and energy balance (Rolland *et al.*, 2002). As a major transport form of sugar, sucrose (Suc) is translocated from source to sink tissues through the phloem and cleaved for its utilization in sink tissues (Kuhn *et al.*, 1999). In plants, Suc utilization is initiated by degradation, either catalysed by sucrose synthase (SUSY; EC 2.4.1.13) or invertases (INV; EC 3.2.1.26). SUSY is located in the cytoplasm and cleaves sucrose reversibly into fructose and UDP-glucose. Invertases exist in several isoforms which exhibit different sub-cellular locations and biochemical properties (Tymowska-Lalanne and Kreis, 1998; Sturm, 1999), and cleave Suc irreversibly to yield glucose and fructose. Vacuolar and cell wall INV (Acid-INV; β-fructofuranosidases of the glycoside hydrolase family 32, Lammens *et al.*, 2009) share some properties, such as their optimum pH (between 4.5 and 5.0) and the K_m values for sucrose which range from 5 mM to 12 mM, displaying maximal activity at 45 °C (Goetz *et al.*, 1999). Plants additionally possess alkaline/neutral INVs (A/N-INV), grouped in the glycoside family 100 (Lammens *et al.*, 2009), with optimal pH in the range of 6.5–8.0 (Tymowska-Lalanne and Kreis, 1998; Sturm, 1999). In contrast to acid invertases, A/N-INV are not glycosylated and do not belong to the β-fructofuranosidase family since they hydrolyse sucrose but no other β-fructose containing sugars (Walker *et al.*, 1997; Sturm, 1999; Sturm and Tang, 1999; Vargas *et al.*, 2003). A/N-INV are located mainly in the cytosol, yet some isoforms are targeted to sub-cellular compartments such as chloroplasts, mitochondria and the nucleus (Murayama and Handa, 2007; Szarka *et al.*, 2008; Vargas *et al.*, 2008).

In *Arabidopsis thaliana*, six and five INV-encoding loci have been functionally characterized as A- and A/N-INV, respectively (Supplementary Table S1). Few reports suggest that cytosolic A/N INV are involved in carbon distribution, cellular differentiation and tissue development, as well as responses to environmental stresses (Qi *et al.*, 2007; Jia *et al.*, 2008; Barratt *et al.*, 2009; Welham *et al.*, 2009; Yao *et al.*, 2009). Reverse genetic experiments using Arabidopsis knockout mutants suggest that the chloroplast-located isoform At-A/N-INVE is involved in the control of carbon balance between the cytosol and plastids, affecting starch accumulation (Vargas *et al.*, 2008). Moreover, another mutant allele of *At-A/N-INVE* led to impairment of photosynthesis and nitrogen assimilation (Tamoi *et al.*, 2010). Xiang *et al.* (2011) showed that mitochondrial *At-A/N INVA* knock-out plants have a more severe growth phenotype than those of cytosolic *At-A/N-INVG* null mutants. The absence of any of these A/N-INV was associated with a higher expression of genes encoding antioxidant enzymes, while transient overexpression of *At-A/N-INVA* and *At-A/N-INVG* in leaf mesophyll protoplasts down-regulated expression of the oxidative stress-responsive *ASCORBATE PEROXIDASE 2* (*APX2*) promoter. Analysis of the Arabidopsis mutant in the mitochondrial *At-A/N-INVC* showed an impaired growth phenotype with a severely reduced shoot growth, with root development not being affected (Martín *et al.*, 2013), similar to that seen in *A/N INVA* knock-out plants (Xiang *et al.*, 2011). More recently, a paper published by Meng *et al.* (2020) demonstrated that CINV(1/2) mediates root growth via a glucose-dependent signaling mechanism. Reduced oxygen consumption was observed in both *At-A/N-INVA* and *At-A/N-INVC* mutants, indicating that they have dysfunctional mitochondria, and suggesting that both isoforms play a fundamental role in the respiratory process (Martin *et al.*, 2013). In rice, when the *OsCyt-inv1* gene, homologous to *At-A/N-INVG* was mutated, plants exhibited short roots, delayed flowering, and partial sterility (Jia *et al.*, 2008). Similarly, in *Lotus japonicus*, mutation in a gene encoding the cytosolic neutral invertase LjINV1 lead to severe reduction of root and shoot growth, blockage of pollen formation and flowering impairment (Welham *et al.*, 2009). Alkaline invertases are also important in response to environmental stresses. Vargas *et al.* (2007) showed that *A/N-INV* expression was up-regulated in wheat leaves upon osmotic stress or low temperature treatments. The above mentioned At-A/N-INVG is also involved in osmotic stress-induced inhibition of lateral root growth by controlling the amount of hexose in cells (Qi *et al.*, 2007).

In tomato (*Solanum lycopersicum*), A-INVs contribute to the determination of important agronomical traits such as fruit soluble solid content (Fridman *et al.*, 2004; Qin *et al.*, 2016), pollen viability and seed size (Zanor *et al.*, 2009), flower and fruit development (Li *et al.*, 2012), and pathogen responses (Kocal *et al.*, 2008). Studies on the roles of A/N-INV have lagged behind. However, some studies suggest important roles for these INVs in tomato: A/N-INV activity has been previously correlated with sucrose import during early fruit growth (Balibrea *et al.*, 2003), and soluble sugar content in ripe fruits (Balibrea *et al.*, 2006). A more recent report described the expression pattern of five A/N-INV encoding loci,

named *NI1-NI5*, across tomato fruit development, and investigated their control by the master transcription factor *Ripening Inhibitor* (*RIN;* Qin *et al.*, 2016).

Prudent *et al.* (2011) have reported the presence of QTLs for sugar supply, metabolic transformation of sugars and dilution of sugars by water uptake in fruits, overlapping a genomic region on chromosome 4. On this same region we have previously identified a putative A/N-INV encoding locus (Kamenetzky *et al.*, 2010), herein named *NI6* following the nomenclature proposed by Qin *et al.* (2016). *NI6* knock-down transgenic plants showed impairments in vegetative growth, flowering and fruit set, greatly impacting on yield penalty. Transcriptome analyses of these plants showed that *NI6* is not only essential for sugar metabolism, but also plays a role in stress adaptation signaling. In addition, these results identify the role of the cytosolic invertase in the redox homeostasis of leaf metabolism, and its impact over carbon export towards sink organs.

Materials and methods

Phylogenetic analysis

For phylogenetic analysis, the Phytozome v10.3 database (Goodstein *et al.*, 2012) was surveyed for *Arabidopsis thaliana* and *Solanum lycopersicum* sequences with homology to Solyc04g081440 and Solyc06g064620 for A- and A/N-INV, respectively. Protein sequences were aligned with the Expresso program (Notredame *et al.*, 2000) using the default parameters. Tree reconstruction was performed by the Neighbour Joining algorithm in MEGA 6.0 (Tamura *et al.*, 2013) with pairwise deletion and the best substitution model found. Branches were supported by bootstrapping following 1000 replications.

Sub-cellular localization

The full-length cDNA of *NI6* (1710 bp) was amplified by PCR using Taq Platinum Pfx DNA polymerase (Invitrogen) and cloned into the binary vector pK7FWG2 (Karimi *et al.*, 2002) by recombination using LR clonase (Invitrogen), resulting in a C-terminal green fluorescent protein (GFP) fusion protein (pK7FWG2-NI6; Supplementary Fig. S1). In-frame fusion and whole sequence fidelity were checked by sequencing. Primer sequences are: F 5' CACCATGCCTAGCCCTGTGGATGTGTC 3' and R 5' ACAAGTCCAAGAAGCAGATCTTTTCATGG 3'. Transient expression via *Agrobacterium tumefaciens* and confocal microscopy examination were performed as previously described (De Godoy *et al.*, 2013).

Generation of transgenic tomato plants

A specific 435 bp fragment of the *NI6* coding region was amplified by PCR (primers; F 5' TGGAAAGGCCAAGACAAGTT 3' and R 5' GCTGGGGACAAAATCTCTGA 3') and cloned into the binary vector pK7GWIWG2(I) (Karimi *et al.*, 2002), as described by De Godoy *et al.* (2013). The vector was introduced in *Agrobacterium tumefaciens* strain GV2260. Seedling cotyledons of *S. lycopersicum* ('Moneymaker') were used as explants to generate transgenic tomato plants with the hairpin construct pK7GWIWG2(I)-NI6. Agrobacterium-mediated transformation was carried out as described previously (Nunes-Nesi *et al.*, 2005). The presence of the transgene was confirmed by PCR with 35S promoter-specific primers (F 5' CCCACTATCCTTCGCAAG 3' and R 5' GCAGGTCACTGGATTTTGG 3'). All the experiments were performed with plants of the T1 generation.

Plant material and growing conditions

Solanum lycopersicum plants were grown in a greenhouse under 16 h/8 h photoperiod, 24±3 °C, 60% relative humidity and a light intensity range of 300±100 μmol $m^{-2}.s^{-1}$. For the *NI6* expression profile experiments, flowers were collected straight after anthesis and fruits at 10, 20, 35, 42, and 55 DAA (days after anthesis) corresponding to fruits at cell division, cell expansion, mature green, breaker and ripe stages, respectively. Mature green fruits were also collected (when the maximum size was reached). Height, width, weight and soluble solid contents (°Brix) were measured with a caliber and refractometer (ATC, Spain), respectively. After three months, aerial biomass was harvested, dried in an oven at 80 °C for 5 d, and weighed. The harvest index was calculated as: total fruit weight ×100/aerial fresh biomass.

Neutral invertase activity assay

Proteins from leaves of four-week old plants harvested in the middle of the light period (between 10 a.m. and 14 p.m.) were extracted using 10× extraction buffer (500 mM HEPES, 100 mM $MgCl_2$, 10 mM EDTA, 10 mM EGTA, 10 mM benzamidine, 10 mM ε-aminocapronic acid, and 10 M KOH to adjust pH to 7.5), 2 mM leupeptin, 500 mM DTT, 100 mM phenylmethylsulfonyl fluoride (PMSF) in isopropanol, 10% (v/v) Triton X-100, 10× glycerol and 20 mg polyvinylpyrrolidone (PVP). Protein concentration was determined using the protein-dye binding method, employing bovine serum albumin as a standard (Bradford, 1976).

Neutral invertase activity was measured by incubating 8 μg of protein at 30 °C in reaction buffer (20 mM HEPES/KOH pH 7.5, 100 mM ultrapure sucrose) and incubating for 1 h without shaking. Tubes containing boiled extracts (95 °C for 7 min) and without sucrose were used as controls. Reactions were stopped by incubating samples at 95 °C for 5 min. Glucose was quantified as described by Stitt *et al.* (1989). Between two and eight biological replicates were made and two technical replicates were performed.

Real-time analysis (qRT–PCR)

Total RNA was extracted from leaves, mature green (35 DAA), and ripe fruits (55 DAA). RNA concentration was determined spectrophotometrically and its integrity checked by running a non-denaturing 1.5% agarose gel. One μg of total RNA was used to synthesize the first-strand of cDNA using Molony murine leukemia virus (MMLV) reverse transcriptase and random primers hexamers, according to the manufacturer's instructions (Invitrogen). The specific primers as well as the Minimum Information for Publication of Quantitative Real-Time PCR Experiments (MIQE) are presented in Supplementary Table S2. Stable expression of the used reference gene (Elongation Factor 1-α, EF1α) under all experimental conditions tested here is also presented as an inset figure in the same Supplementary Table S2.

PCR conditions were as follows: 95 °C for 5 min, 40 cycles at 95 °C for 15 s, 60 °C for 60 s and a final extension at 72 °C for 30 s in an Applied Biosystems Step One Plus Real Time. Data analysis and primer efficiencies were obtained using LinRegPCR (Ramakers *et al.*, 2003). Statistical analysis were performed using fgStatistics (Di Rienzo *et al.*, 2016). Six to eight biological replicates were used with two technical replicates.

Photosynthetic parameters

Gas exchange measurements were performed with LI-6400XT (LiCor Inc.; Lincoln, Nebraska). Except for light intensity, the measurement chamber conditions were chosen to be similar to those surrounding the plant inside the greenhouse (400 μmol mol^{-1} CO_2 concentration, leaf temperature of 23±0.5 °C and relative humidity set between 55–75 %),

with the air flow set at 500 µmol s^{-1}. Photosynthetically active illumination (90% red light/10 % blue light) was provided by the LI6400-40 instrument. Before measurements begun, leaves were equilibrated in the measurement chamber for 10 min at a light intensity 100 µmol photons m^{-2} s^{-1}. Once a steady state was reached, light intensity was increased to 1200 µmol photons m^{-2} s^{-1}, and was decreased stepwise to 1000, 800, 400, 200, 100, 50 µmol photons m^{-2} s^{-1}, with a final recording in the dark to compute respiration rates. Gas exchange parameters were recorded at each light intensity only when a steady maximum was obtained (approximately 5 min).

Determination of soluble sugars and starch

Soluble carbohydrates were extracted from leaf samples of four-week old plants taken during a time course of 24 h every 3 h or 4 h. Twenty mg of tissue from each time point were extracted twice in 80% ethanol and once in 50% ethanol. Thirty µl of the extract was used to determine hexoses and sucrose, as describe by Stitt *et al.* (1989). In fruits, soluble carbohydrates were extracted from 100 mg of tissue, as previously described (Carrari *et al.*, 2006). Five independent extractions from five biological replicates were made and two technical replicates of each biological sample were performed.

Starch was extracted from remaining pellets after soluble carbohydrate extraction from 100 mg and 250 mg of leaves and fruits, respectively. The pellet was washed with 0.5 ml of 40 % ethanol and resuspended in 0.4 ml of 0.2 M KOH. After 1 h at 95 °C, 0.07 ml of 1 M acetic acid was added. Following this, 12.5 µl of the extract was incubated at 56 °C for 45 min with 25 µl of starch assay solution 1 (Sigma-Aldrich), and 25 µl of this sample was measured with 175 µl of glucose (HK) assay solution 2 (Sigma-Aldrich). Glucose content was measured as described by Stitt *et al.* (1989). Five independent extractions from five biological replicates were made.

Sucrose, glucose, and fructose content in flowers collected at the first day of anthesis were analysed according to the method described by Wilson *et al.* (1981) with minor modifications. Briefly, 200 mg of material were ground in 5 ml of 80% (v/v) ethanol, followed by incubation for 30 min at 80 °C and centrifugation at 15 000 × *g* for 30 min, then repeated with 80% (v/v) ethanol. The supernatant was evaporated and re-suspended with 3 ml double-distilled water. After filtering through a 0.45 µm microfiltration membrane, the sucrose, glucose and fructose content in supernatants were analysed on Waters Alliance equipment (Waters) coupled with a NH2 column (using the HPLC method).

Gas chromatography-mass spectrometry

Samples from two different experiments were analysed. Leaves, mature green fruits and ripe fruits were harvested from the same experiment described above. Frozen tissues (80 mg) were extracted with 990 µl of 100 % methanol, with 20 µl of ribitol as an internal standard (0.2 mg ml^{-1}) for data normalization. The samples were extracted for 15 min at 70 °C, mixed vigorously with 450 µl of water, centrifuged at 2200 × *g* and subsequently reduced to dryness under vacuum. The residue was re-dissolved and derivatized for 120 min at 37 °C (in 60 ml of 30 mg ml^{-1} methoxyamine hydrochloride in pyridine) followed by a 30 min treatment at 37 °C with 120 ml of *N*-methyl-*N*-[trimethylsilyl] trifluoroacetamide. Sample volumes of 1 µl were then injected in split-less and split modes, using a hot needle technique. The gas chromatography–time-of-flight–mass spectrometry (GC-tof-MS) system was composed of an AS 2000 autosampler, a GC 6890N gas chromatographer (Agilent Technologies, USA), and a Pegasus III time-of-flight mass spectrometer (LECO Instruments, USA). Mass spectra were recorded at 20 scans s^{-1} with a scanning range of 70 to 600 m z^{-1}. Both chromatograms and mass spectra were evaluated using ChromaTOF, chromatography processing and mass spectral deconvolution software, version 3.00 (LECO Instruments, USA). Identification and quantification of the compounds were performed with TagFinder 4.0 (Luedemann *et al.*, 2008) and the mass spectra were cross referenced with those in the Golm Metabolome Database. Four biological replicates were used for this analysis.

RNA-seq data analyses

Total RNA from leaves of four independent biological replicates of each line (pools of two plants each) were extracted using Trizol (Invitrogen). RNA quality was assessed with a Bio Analyzer 2100 (Agilent Technologies), and RNA concentration was determined with a spectrophotometer (Nanodrop ND-1000; NanoDrop Technologies, Wilmington, DE, U.S.A.). RNA libraries were constructed by LC Science Company following the recommendations in the Illumina kit (Directional mRNA-Seq Sample Preparation, Illumina). For sequencing, eight libraries were pooled in one lane of a flow cell. The library products were sequenced using a HiSeq2500 sequencing system (Illumina). Cluster preparation and single-ends read sequencing were performed according to the manufacturer's instructions. Processing, mapping of RNA-sequencing reads and statistical procedures for analysing the raw sequencing reads generated for differentially expressed genes were initially processed and quality trimmed with FastX-ToolkitV0.0.14 (http://hannonlab.cshl.edu/fastx_toolkit/). Briefly, for primer trimming a minimum adapter alignment of 25 bp was used, for quality trimming we required a quality score to keep 20 bp considering a minimum percentage of bases of 95 %, discarding sequences shorter than 30 bp. After this process, we obtained 150 million clean reads (80% raw data) with an average of 30 million clean reads by sample with an average read length of 50–75 bp. The remaining cleaned and high quality reads were then aligned to the tomato genome (ftp://ftp.solgenomics.net/tomato_genome/annotation/ITAG2.4_release//) using Bowtie2/v.2.2.2 (Langmead and Salzberg, 2012) allowing one segment mismatch (Trapnell *et al.*, 2009). Only those reads uniquely mapping to the reference data set were subsequently used for analyses. All RNA-seq data were analysed and visualized in R version 3.1.3 (R Core Team, 2015) with cummerRbund package version 2.8.2 (Goff *et al.*, 2012) using the normalized FPKM (fragments per kilobase of transcript per million reads). Empirical analysis of differential gene expression was done by Cufflinks v2.2.1 (Trapnell *et al.*, 2012) using a False Discovery Rate (FDR) ≤5% cut-off and a $\log_2$ fold change ≥1. Category enrichment analysis was performed by the Mercator web application (Lohse *et al.*, 2014).

Enzymatic activities

Desalted extracts were used to measure selected enzymes using spectrophotometric assays. Apoplastic invertase activity was measured as described by Baxter *et al.* (2005). Pyruvate kinase activity was measured as in Gibon *et al.* (2004). Suc synthase (hydrolytic direction) was determined as detailed by Zrenner *et al.* (1995). ADP-glucose pyrophosphorylase (AGPase) activity was measured in the pyrophosphorolysis direction with a spectrophotometric assay, as described previously (Tiessen *et al.*, 2002; 2003). AGPase activity was measured in the ADP-glucose-cleaving direction in the absence (Vsel) or presence of dithiothreitol (Vred). The ratio between the activities in these two assays (Vsel/Vred) is termed 'activation state'.

Integration of metabolite and transcript data

To integrate transcriptomic and metabolic data, a Pearson rank correlation was performed between 472 differentially expressed genes (DEGs) detected in at least two transgenic lines plus those genes identified as eingen vectors showing values above the average in a principal component analysis (PCA) and all the metabolites detected and quantified in the

metabolomics analysis shown in Supplementary Table S3. Pearson correlations were computed using Infostat (Di Rienzo *et al.*, 2016). Variables with a pair-wise association score greater than |0.84| and $P<0.01$ were selected as first criterion (462 genes and 20 metabolites). A second-level criterion was the selection of two gene categories: gene 1 (G1); those showing at least one connection with one metabolite and gene 2 (G2); those connected to G1. A total of 322 and 140 genes were identified as G1 and G2, respectively. Moreover, for the case of metabolites, those showing at least one connection (20 metabolites; either with G1 or with another metabolite) were included for further analyses (Supplementary Table S4). Finally, out of this selection and to draw the relevant network generated with Cytoscape Package (Shannon *et al.*, 2003), we chose only those genes varying in all three transgenic lines (Supplementary Table S5) with all their metabolite connections. The size of a node in the network reflects its degree of connectivity and the color indicates the functional Mapman category for each locus (represented as circles), as detailed in Supplementary Table S6; metabolites are indicated as light-green squares. Edge colors represent the sign of the correlation coefficients (blue=negative, red=positive).

Results

Invertase gene family in tomato

Although a recent publication gave a different ID to the Solyc04g081440 locus previously identified by Kamenetzky *et al.*, (2010) (*SlCIN01;* Pan *et al.*, 2019), herein we designated it as *NI6*, following the numerical nomenclature previously proposed by Qin *et al.* (2016). We thus concentrated on the diversity of genes encoding invertases and explored the group of INVs containing *NI6*. A survey in the Arabidopsis and *S. lycopersicum* genomes, followed by a phylogenetic reconstruction of the protein sequences, led to the identification of 15 and 20 invertase encoding loci, respectively (Supplementary Table S1). The phylogeny obtained from the alignment of the 35 amino acid sequences revealed two clear clades; one grouping A-INV and the other grouping A/N-INV (Fig. 1A). In each clade, groups could be recognized according to the sub-cellular localization of the proteins. Thus, A-INV clade was divided into one group of vacuolar and another of cell wall-localized proteins, while the A/N-INV contained three groups, namely mitochondrial, plastidial and cytosolic invertases.

In tomato, we found 20 genes encoding INV (Supplementary Table S1), 12 encoding A-INV, and eight encoding A/N-INV. This finding extended the INV catalog recently reported by Qin *et al.* (2016), which published the existence of six A-INV and five A/N-INV. Moreover, the robust tree topology allowed us to clearly predict the sub-cellular localization of the proteins encoded by the 20 tomato loci (Fig. 1A). NI6 was found to belong to the A/N-INV clade, clustering within the cytosolic invertases. This cytosolic localization was further confirmed by confocal microscopy analysis of tobacco leaves transiently expressing the NI6::GFP fusion protein (Fig. 1B).

Interestingly, according to the data available in TomExpress (http://gbf.toulouse.inra.fr/tomexpress/www/welcomeTomExpress.php), the six A-INV identified in tomato seemed to be expressed in low amounts in leaves and fruits (Supplementary Table S1). By contrast, except for the case of the Solyc01g111100 locus, all *A/N-INV* genes showed detectable expression (Supplementary Table S1), according to the qPCR analyses shown in Fig. 1C for leaves and fruits. *NI6* was the most expressed *A/N-INV* gene in fruits at mature green stage, while Solyc11g007270 was the locus with the highest expression in leaves and ripe fruits (Fig. 1C). Moreover, a detailed tissue-specific qPCR profile showed that *NI6* was expressed in all tomato organs tested (leaves, stems, flowers and fruits), with peak expression in mature green fruits (Supplementary Table S7).

Generation and selection of NI6 *knock-down plants*

In order to determine the physiological role of *NI6* in tomato, we followed a RNA interference (RNAi) approach to generate constitutively silenced transgenic plants. Out of 26 independent transgenic lines, six showed significant reductions in A/N-INV activity in source leaf extracts (Fig. 2A), and lines 20, 26, and 30 were selected for further analysis. To demonstrate that these reductions in activity were the consequence of the reduction in *NI6* expression, we evaluated expression of this gene by qPCR (Fig. 2B) in six to eight plants per line, and in three different organs: source leaves, mature green, and ripe fruits. In all cases, *NI6* expression was less than 10% in the transgenic lines with respect to the amounts found in the wild-type controls.

NI6 *knock-down causes impairment in plant growth, flowering, and fruit set*

In order to assess the effect of the *NI6* knock-down on growth and development of tomato plants, detailed phenotypic analyses were performed. We analysed six-week old plants from selected transgenic lines (Fig. 3A). At this stage, differences in size between the *NI6* knock-down and wild-type lines were remarkable, and this was due to shorter internodes and a lower growth rate. At the flowering stage, it was noteworthy that the transgenic plants produced fewer flowers, most of which aborted, resulting in a dramatic reduction in fruit set. Even though there was not a large difference compared with wild type, average weight of the mature fruits in transgenic lines decreased significantly (*t*-test; $p<0.05$) (Fig. 3B).

Notwithstanding the differences in plant growth observed at the beginning of development described above, biomass accumulation in the aerial vegetative tissues (leaves and stems) after 16 weeks of growth was invariant between genotypes (Fig. 3C). However, both flower abortion and the reduction in fruit set observed in the silenced lines had a tremendous impact on the harvest index. Finally, we observed that ripe fruits displayed higher values of soluble solids (°Brix) relative to the wild type (Fig. 3C).

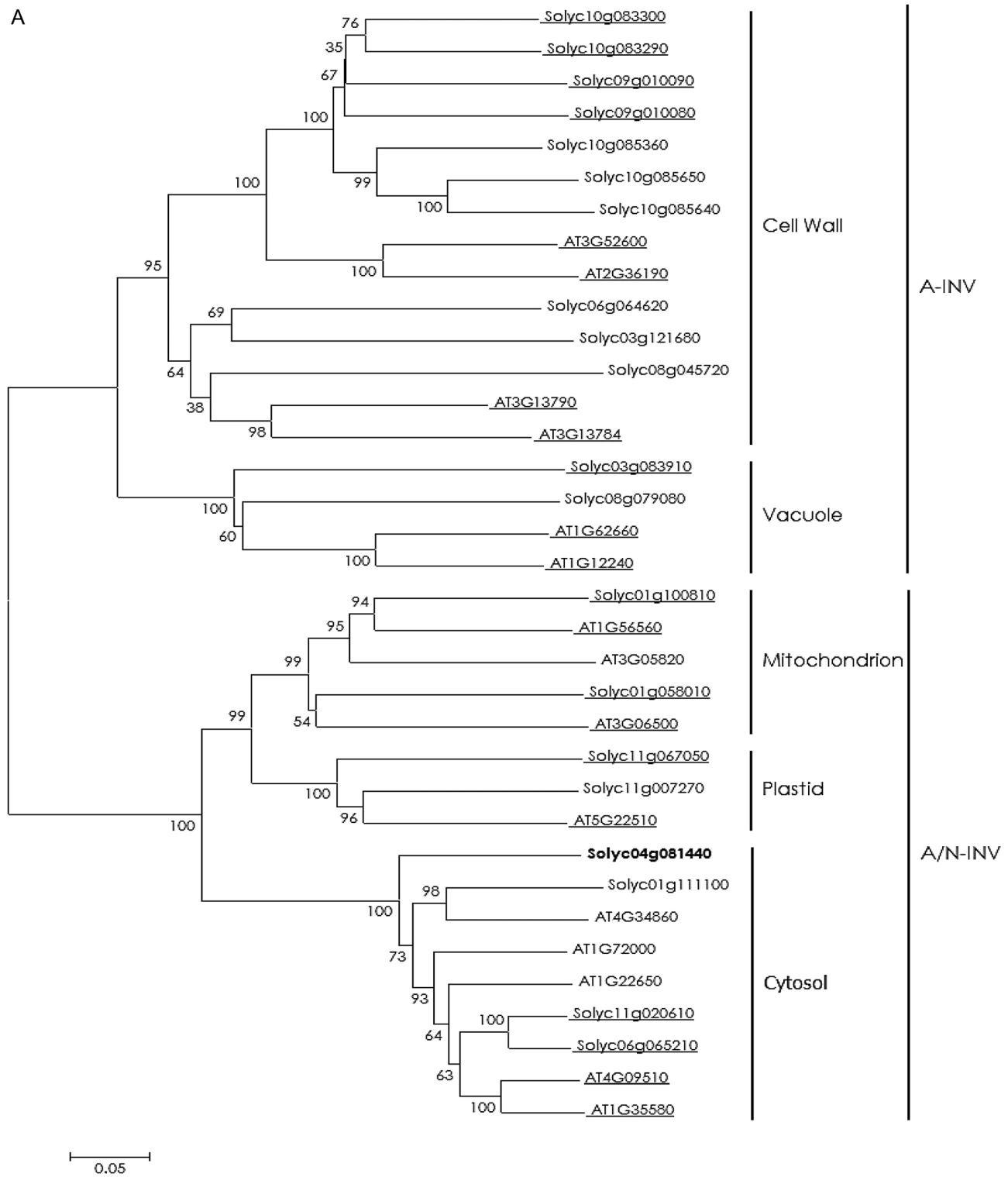

Fig. 1. Invertase gene family in tomato. (A) Phylogenetic analysis of the A- and A/N- INV identified in Arabidopsis and tomato genomes. Sequences were obtained from Phytozome database (Supplementary Table S1). Tree topology reveals groups with distinct sub-cellular localizations within each clade. Underlined loci are those for which functional characterizations are published and *NI6* locus (Solyc04g081440) is highlighted in bold. (B) Confocal images of *N. tabacum* mesophyll cells expressing HPPD:GFP (hydroxyphenylpyruvate dioxygenase, a cytosolic control; top panel) or NI6:GFP (bottom panels; two independent cells transiently expressing NI6:GFP fusion) fusion proteins. GFP, chlorophyll fluorescence, and merged signals are indicated above the panels. Bar, 20 μm. (C) A/N-INV paralogs expression in tomato leaves, mature green and ripe fruits from wild type tomato plants ('M82'). Bars indicate means ±SE from three to six biological replicates. * denote statistically significant differences compared with NI6 expression (*t*-test; $P<0.05$).

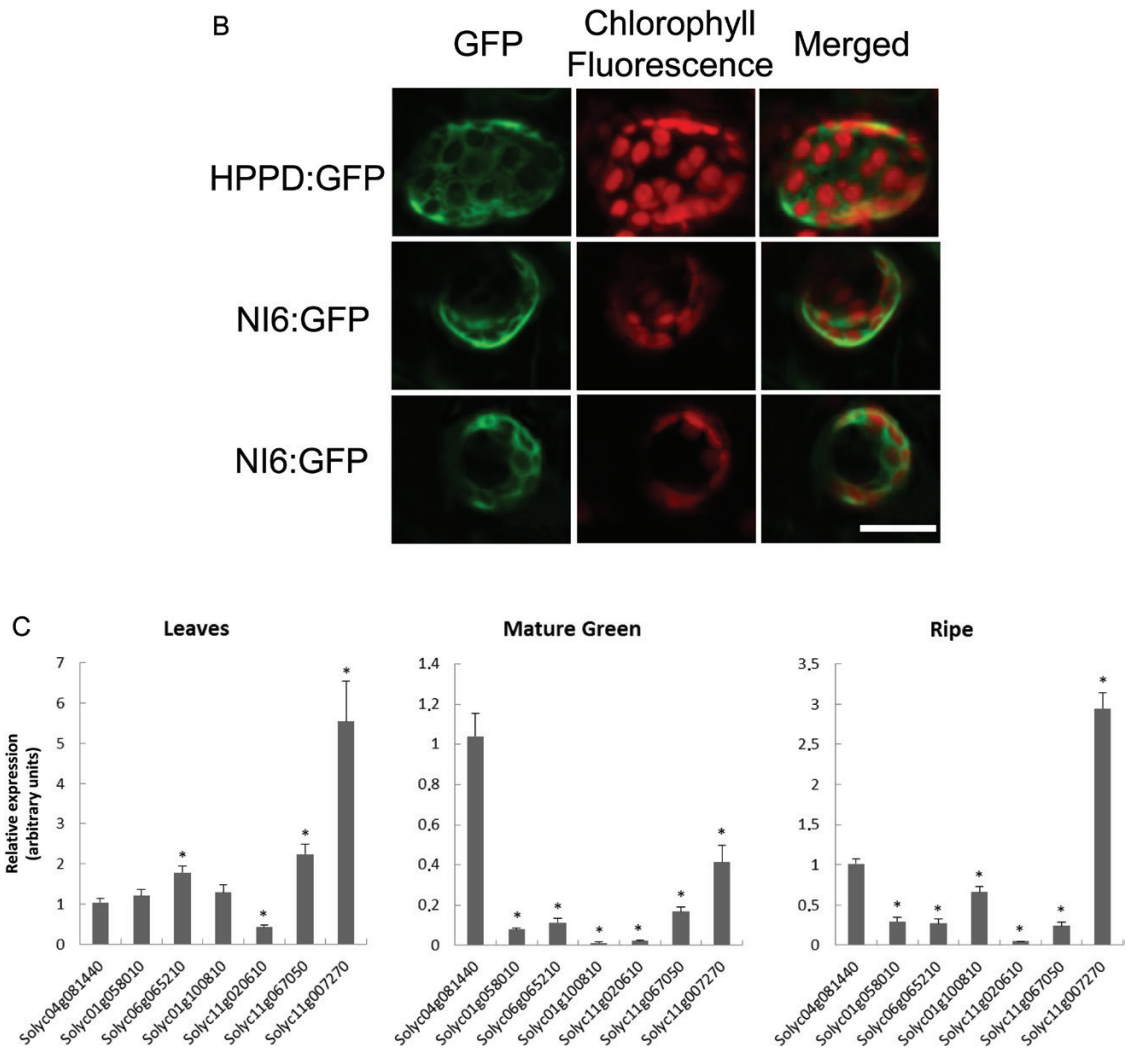

Fig. 1. Continued.

Metabolic alterations as a consequence of NI6 *silencing*

The amount of soluble carbohydrates was evaluated through a diurnal period in source leaves from four-week old plants. Only the leaves from line 30 showed significant increases (*t*-test; $p<0.05$) in the contents of both glucose (Glu) and fructose (Fru) at 12 h, 16 h and 20 h, while line 26 showed a significant decrease in Fru content at 12 h, in contrast with wild-type controls (Fig. 4A, B). *NI6* knock-down lines accumulated more sucrose at certain points of the time course (Fig. 4C). Starch content, measured at the middle of the light period, decreased in lines 20 and 26 (Fig. 4D). Moreover, at the end of the day, it was significantly reduced in lines 26 and 30. This lower starch content can be explained by the reduced amounts of AGPase activity (in its activation state) found in the transgenic lines (Table 1). No alterations were detected in the activities of soluble acid invertase and sucrose synthase (Table 1). Overall, the soluble sugar and starch profiles reflect an altered pattern of carbon distribution in the transgenic plants.

In order to gain a deeper understanding of the metabolic basis related to changes in major sugars and in the above described differences in growth and development of the *NI6* silenced plants, we next determined metabolite concentrations in source leaves harvested at the middle of the light period. We applied an established gas chromatography-mass spectrometry (GC-MS)-based metabolite profiling method (Roessner-Tunali *et al.*, 2004). Source leaves from four-week old transgenic lines were characterized by increases in the amounts of saccharate, quinate, asparagine, phosphorate, glucose, fructose, γ-aminobutyric acid (GABA), and glycine, and reductions in dehydroascorbate, pyroglutamate, phenylalanine, valine, serine, and tyramine (Supplementary Table S3). Principal component

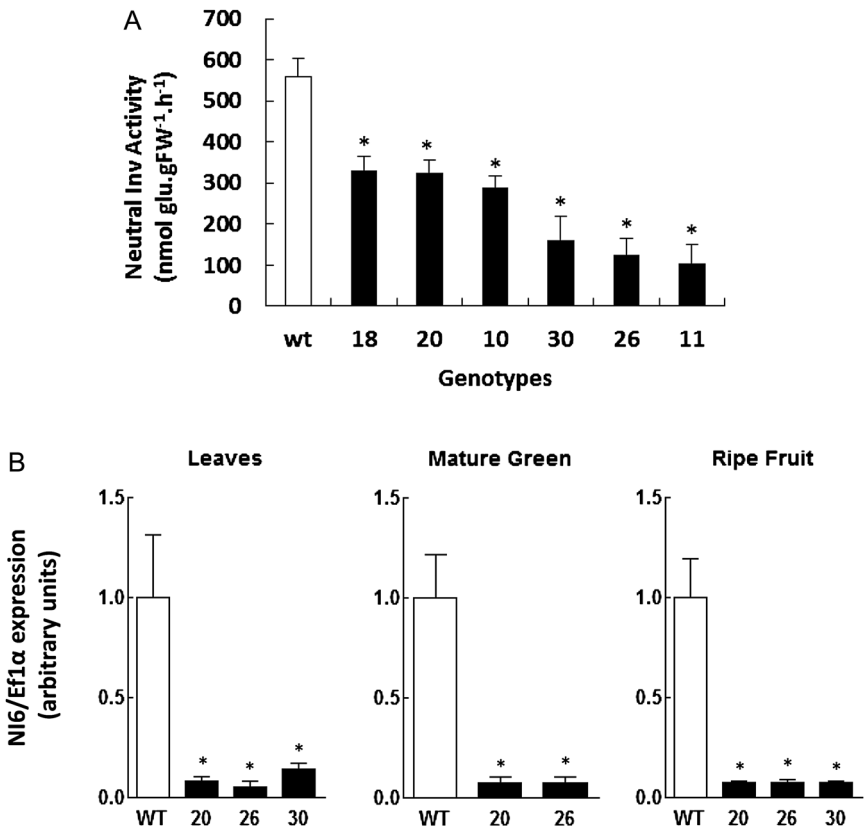

Fig. 2. Analyses of *NI6* silenced lines. (A) Screening of transgenic lines by A/N-INV activity measurements in source leaves from eight plants per genotype. (B) *NI6* expression in source leaves, mature green, and ripe fruits from the selected lines in (A) quantified by qRT–PCR. Bars indicate means ±SE from six to eight plants per genotype. * denote statistically significant differences compared with the wild type controls (*t*-test; $P<0.05$). Due to the fruit impairment of the transgenic lines, *NI6* expression was not assayed in mature green fruits from line 30.

analysis of these data explained about 40% of the variance and even when the replicates from the transgenic lines scattered over the two first components, they were separated from the wild-type ones (Fig. 4E). In summary, these analyses showed that *NI6* silencing not only affected the amounts of major sugars and the pool of most of amino acids, but also modified the cellular redox status.

Considering the high flower abortion rate, we next measured soluble sugar content in this organ (at first day of anthesis). This analysis showed that Suc content was significantly (*t*-test; $p<0.05$) reduced in the flowers of the transgenic lines (as well as Fru amounts in one of the transgenic lines; Table 2).

NI6 *silenced plants display penalty in photosynthesis*

The effect of *NI6* silencing on foliar gas exchange parameters was evaluated at different photon flux densities (PFD) in four-week old plants (Supplementary Table S8). Lower rates of CO_2 assimilation and stomatal conductance were observed for lines 20 and 30 at 800 and 1200 µmol photons m^{-2} s^{-1}, while no significant differences were seen in the transpiration rate compared with the wild types. This mild reduction of photosynthesis can be explained by a repression effect exerted by the increased amounts of glucose in the leaf of the transgenic plants (Jang *et al.*, 1997).

Global gene expression analysis in leaves from NI6 *silenced plants*

In order to better understand the molecular mechanisms underneath the growth, developmental and metabolic alterations identified in *NI6* knock-down plants, we profiled the expression of source leaves from four-week old plants in an RNA-seq experiment. A total of 19 937 loci were detected in both replicates for at least one of the genotypes (Supplementary Table S9). Principal component analysis of this set of data was able to clearly separate the wild type control plants from the transgenic ones in the two first dimensions, which encompassed 46% of the total variance at the transcript level (Fig. 5A). The number of differentially expressed genes (DEGs) compared with the wild type controls were common to the three transgenic lines analysed (Fig. 5B). Twenty seven and 67 genes were down- and up-regulated respectively, as a consequence of *NI6* silencing (Supplementary Table S5). Although these 94 common DEGs belong to a number of MapMan categories

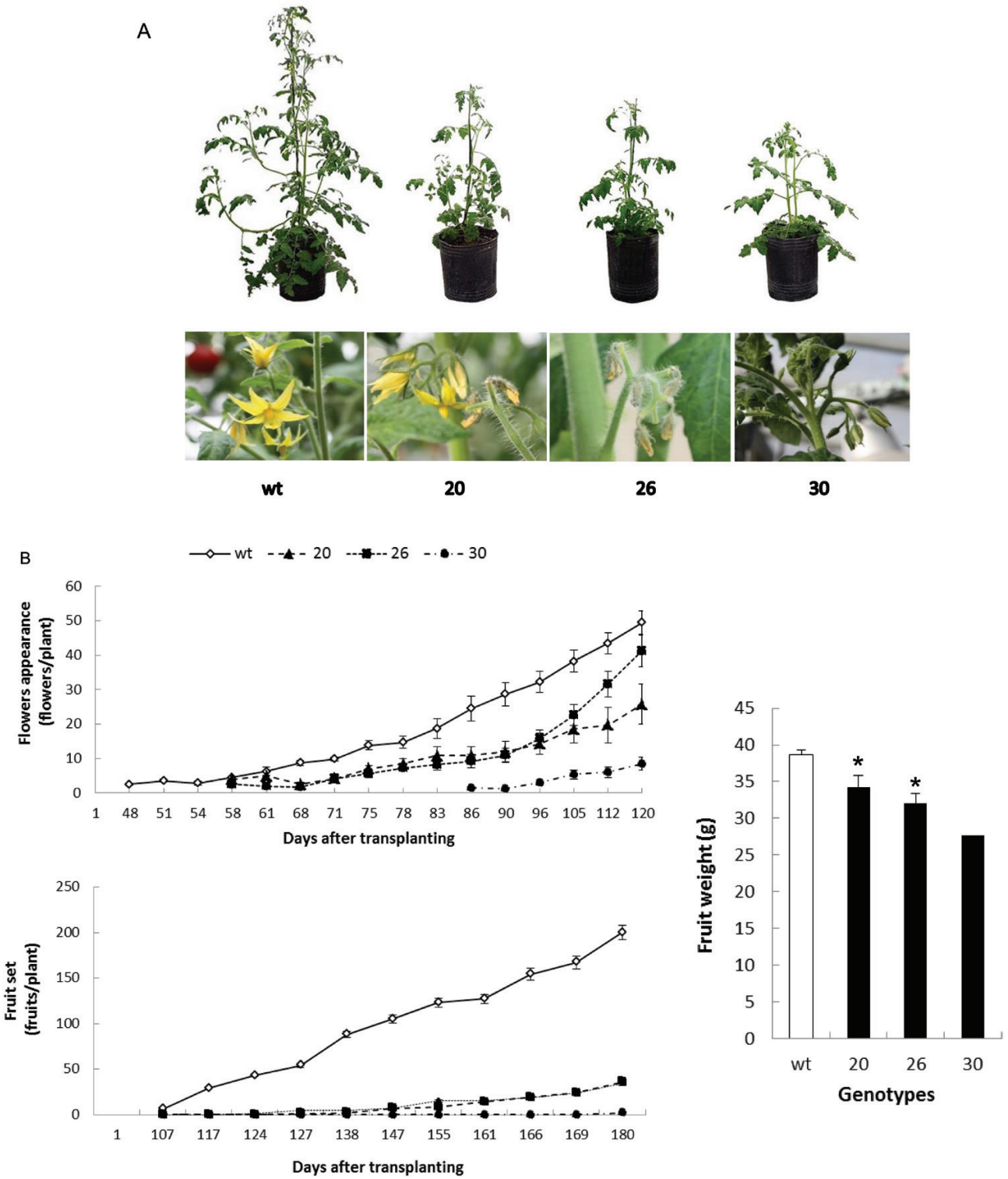

Fig. 3. Phenotypic characterization of the *NI6* knock-down plants. (A) Images of six-week old plants (in vegetative stage) and their corresponding flowers. (B) Flower appearance and fruit s*et al*ong plant development and average weight of the fruits at harvest time. (C) Dried matter accumulation in leaves and stems of 16 week-old plants. Harvest index calculated as total fruit weight × 100/aerial biomass in plants of eight to 10 weeks. Soluble solid content (°Brix) was measured in ripe fruits. Rate of fruit abortion was calculated as a percentage. Bars indicate means ±SE from five individuals of each line. * denotes statistically significant differences compared with the wild type (*t*-test; $P<0.05$).

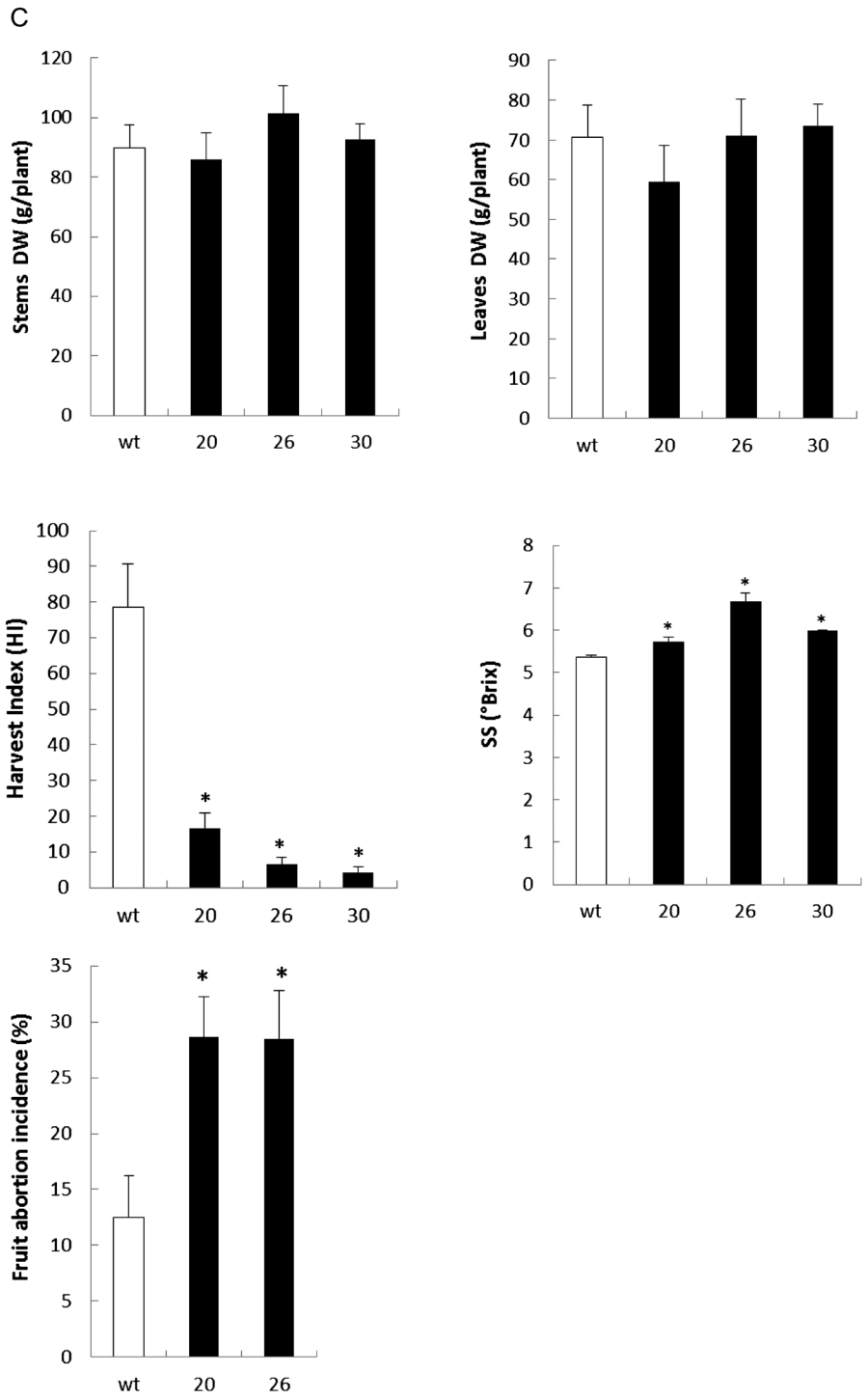

Fig. 3. Continued.

(Urbanczyk-Wochniak *et al.*, 2006; Fig. 5C), only the following categories were found to be over-represented when a contingency test ($P<0.01$) was applied: signaling (30), protein (29) and RNA (27). Intriguingly, protein degradation-associated genes (10 out of 23 up-regulated genes) and genes encoding receptor-like kinases were highly abundant, totaling 17 out of the 94 DEGs. Of note is the up-regulation of the gene encoding extracellular invertase LIN6 . This locus showed two to four-fold fold change (FDR<0.01) in the leaves of the transgenic lines.

Overall, the comparative analysis of the transcript profiles supports a pivotal role of *NI6* in linking sugar metabolism with

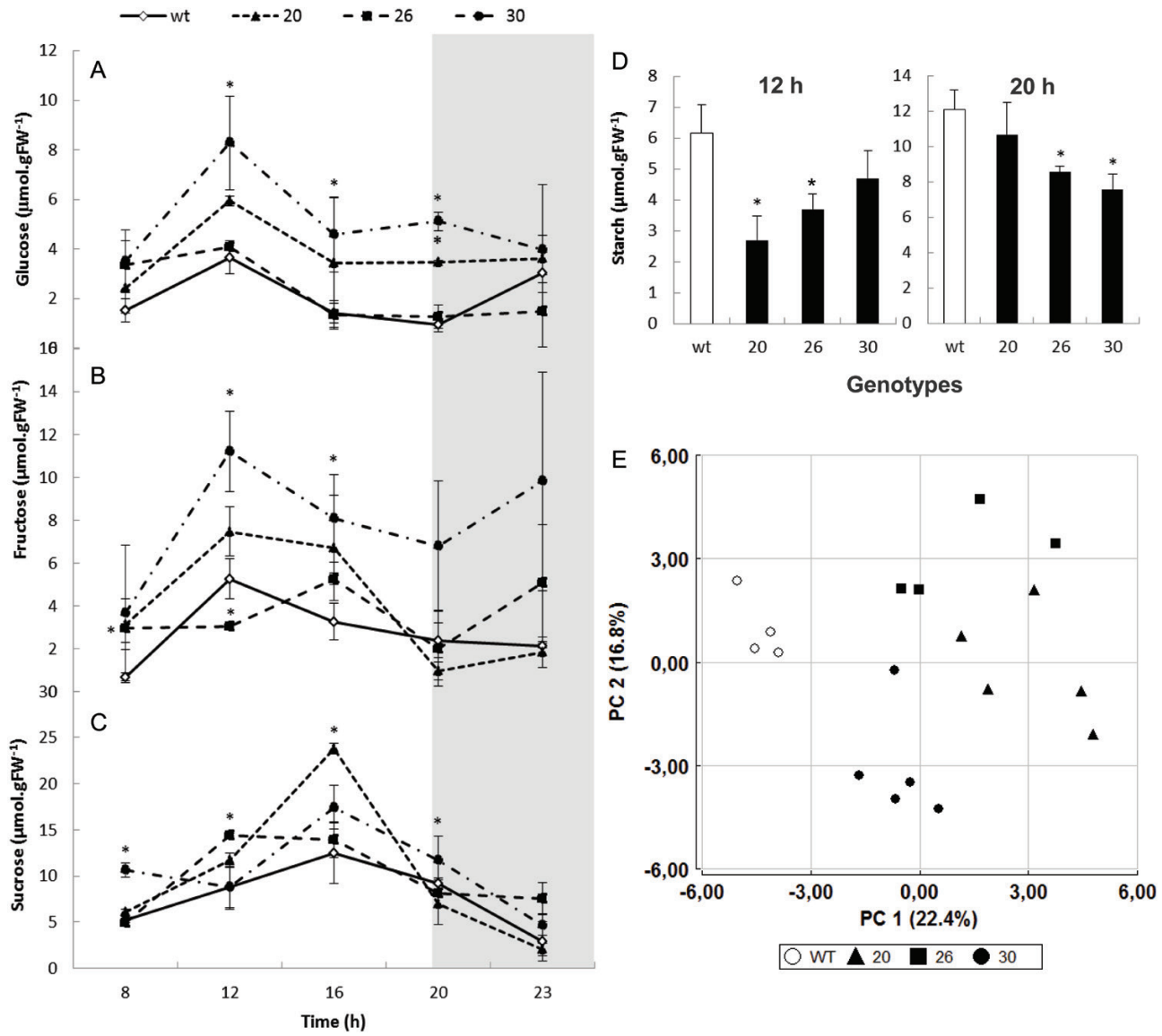

Fig. 4. Metabolic alterations of *NI6* silenced plants. Diurnal time course of glucose (A), fructose (B), and sucrose (C) in leaves collected from four-week old plants. (D) Starch content was measured in leaves from the same plants harvested at the middle (12 h) and at the end (20 h) of the light period. (E) Principal Component Analyses of primary metabolites measured by GC-MS in source leaves collected from the same plants at the middle of the light period. Samples were taken from mature source leaves and data represent the mean of measurements ±SE from four to five plants per genotype. *denote statistically significant differences compared with the wild type (*t*-test; $P<0.05$).

Table 1. Enzymes activities in leaves of the *NI6* silenced lines.

Enzymatic activity	WT	20	26
AGPase + PGA (nmol min^{-1} g^{-1} FW)	678.65±10.53	**431.67±7.34**	**528.37±11.36**
AGPase - PGA (nmol min^{-1} g^{-1} FW)	466.27±8.44	**321.36±12.48**	**398.29±14.12**
AGPase activation state (Vsel/Vred)	0.78±0.06	**0.58±0.1**	**0.64±0.04**
Soluble acid invertase (µmol min^{-1} g^{-1} FW)	1.76±0.09	1.84±0.06	1.69±0.08
Neutral invertase (µmol min^{-1} g^{-1} FW)	5.65±0.06	**3.67±0.09**	**3.76±0.13**
Sucrose synthase (nmol min^{-1} g^{-1} FW)	35.78±2.89	37.63±2.78	32.11±2.54

Data represent means of five replicates ±SE. Numbers in bold indicate statistically significant differences in comparison to the wild type line (*t*-test; $P<0.05$).

Table 2. Soluble sugar content in flowers (first day of anthesis) of the *NI6* silenced lines.

	WT	20	26
Sucrose (mg g^{-1} FW)	6.4±0.4	**4.3±0.6***	**5.3±0.5***
Glucose (mg g^{-1} FW)	2.4±0.3	2.0±0.2	2.5±0.3
Fructose (mg g^{-1} FW)	2.9±0.3	**2.0±0.2***	2.4±0.3

Data represent means of five replicates ±SE. Numbers in bold and asterisks indicate statistically significant differences in comparison to the wild type line (*t*-test; $P<0.05$).

cellular processes such as kinase signaling pathways and RNA and protein metabolism.

Integrated analyses of gene expression and metabolite profiling in leaves from NI6 *silenced plants*

For the purpose of a transcript-metabolite integration analysis, Pearson rank correlations were evaluated. After applying a very stringent selection (Material and Methods; Supplementary Table S4), 800 edges (111 gene-metabolite; 676 gene-gene; 13 metabolite-metabolite) involving 112 nodes (92 genes and 20 metabolites) were identified (Fig. 6). The proportion of genes connecting metabolites (G1) was higher than those connecting other genes (G2). This was true either for the entire set of correlations (322 G1 versus 140 G2) or for the selected network shown in Fig. 6 (57 G1 versus 35 G2). In this, *NI6* is connected with eight genes but with no metabolite. Four of these genes encode signaling proteins such as integrin kinases (G22 and G198) and another two types of kinase proteins (G445 and G448). Interestingly, the gene encoding extracellular invertase LIN6 (neither G1 nor G2) showed 104 connections with genes of the above-mentioned overrepresented categories: protein degradation-associated and receptor-like kinases (Supplementary Table S4).

Based on the type of connections it was possible to differentiate two main clusters, S and B, including 40 and 53 genes, respectively. These two clusters are connected to each other by negative correlations and were identified depending on the metabolite(s) they were linked to. Two groups of metabolites/hubs were recognized: (i) those correlating positively and negatively with cluster S and B, respectively (dehydroascorbate, tyramine, phenylalanine and pyroglutamate), and (ii) those correlating negatively (glutamate) or positively (asparagine, maltose, threonine, phosphate and glycine) exclusively with cluster B. In terms of the kind of genes falling into each cluster, B showed an enrichment in G1, compared with G2 (77 % versus 23 %).

Discussion

The general importance of invertases has been well documented in Arabidopsis (Barratt *et al.*, 2009), and few reports document their significance as possible targets of selection in tomato (Sauvage *et al.*, 2014) and/or describe metabolic engineering approaches in crop species (Sonnewald *et al.*, 1997; Fridman *et al.*, 2004; Jin *et al.*, 2009; Zanor *et al.*, 2009). In particular, the importance of A/N-INVs has only been recently recognized since the catalytic mechanism of a cyanobacterium enzyme was reported (Xie *et al.*, 2016; Wan *et al.*, 2017). These invertases appear to have been acquired by plants via endosymbiotic gene transfer (Vargas *et al.*, 2003). However, the physiological role of A/N-INV for the whole plant is still being investigated (Qi *et al.*, 2007; Vargas *et al.*, 2008; Xiang *et al.*, 2011; Martín *et al.*, 2013).

In carrying out a detailed survey of the tomato genome, we found 20 loci, distributed across eight of the 12 chromosomes, encoding 12 and eight A- and A/N-INV, respectively (Supplementary Tables S1 and Fig. 1A). None of the latter had been previously studied when Qin *et al.* (2016) showed the expression pattern of *NI1-5* during tomato fruit ripening, and a detailed evolutionary study was recently reported by Wan *et al.* (2018). Both our phylogenetic and NI6:GFP transient expression analyses confirmed that NI6 belongs to the β group of A/N-INV which localize in the cytosol (Fig. 1A and 1B). Moreover, *NI6* mRNA was expressed in all organs of the tomato plants (Supplementary Table S7) and its silencing severely affected the vegetative growth (Fig. 3) and the transcriptional regulation of signaling, protein and RNA-related genes (Fig. 5C). In particular, silenced plants showed shorter internodes and transcriptomic data support an involvement of gibberellin signaling as various members of the Snakin/GASA gene family and the gibberellin receptor GID1L2 (Nahirñak *et al.*, 2012) showed altered expression in the transgenic plants (Supplementary Fig. S2). These pieces of evidence demonstrate that NI6 plays a fundamental role in controlling cytosolic sugar homeostasis and also suggest a role in the signaling network that orchestrate gene expression. This is in line with the fact that the β group of A/N-INV is more evolutionary conserved than the α ones, the latter being organelle-associated A/N-INV (Wan *et al.*, 2018). However, we cannot rule out the possibility that transcriptional changes observed in the transgenic lines are the result of a metabolic perturbation displayed by these plants.

Moreover, *NI6* silencing showed dramatic effects on flowering time which was very detrimental for fruit setting. This latter phenotype is a consequence of the high amount of flower abortion observed in the knock-down lines (Fig. 3A and 3B). These results are in agreement with the influential mechanism that the cell wall and soluble invertases have in controlling normal sugar uptake by the ovaries described for maize flowers (Boyer and McLaughlin, 2007), and the differential role of the cell wall A-INV during pollination and fertilization in tomato flowers (Shen *et al.*, 2019). Down-regulation of these enzymes depleted ovary sugar pools and resulted in an up-regulation of senescence-associated genes, triggering cell membrane degradation and thus, irreversible flower abortion (Boyer and McLaughlin, 2007). Although there is sufficient evidence linking A-INV to the normal development of flowers and fruits in tomato (Zanor *et al.*, 2009; Li *et al.*, 2012;

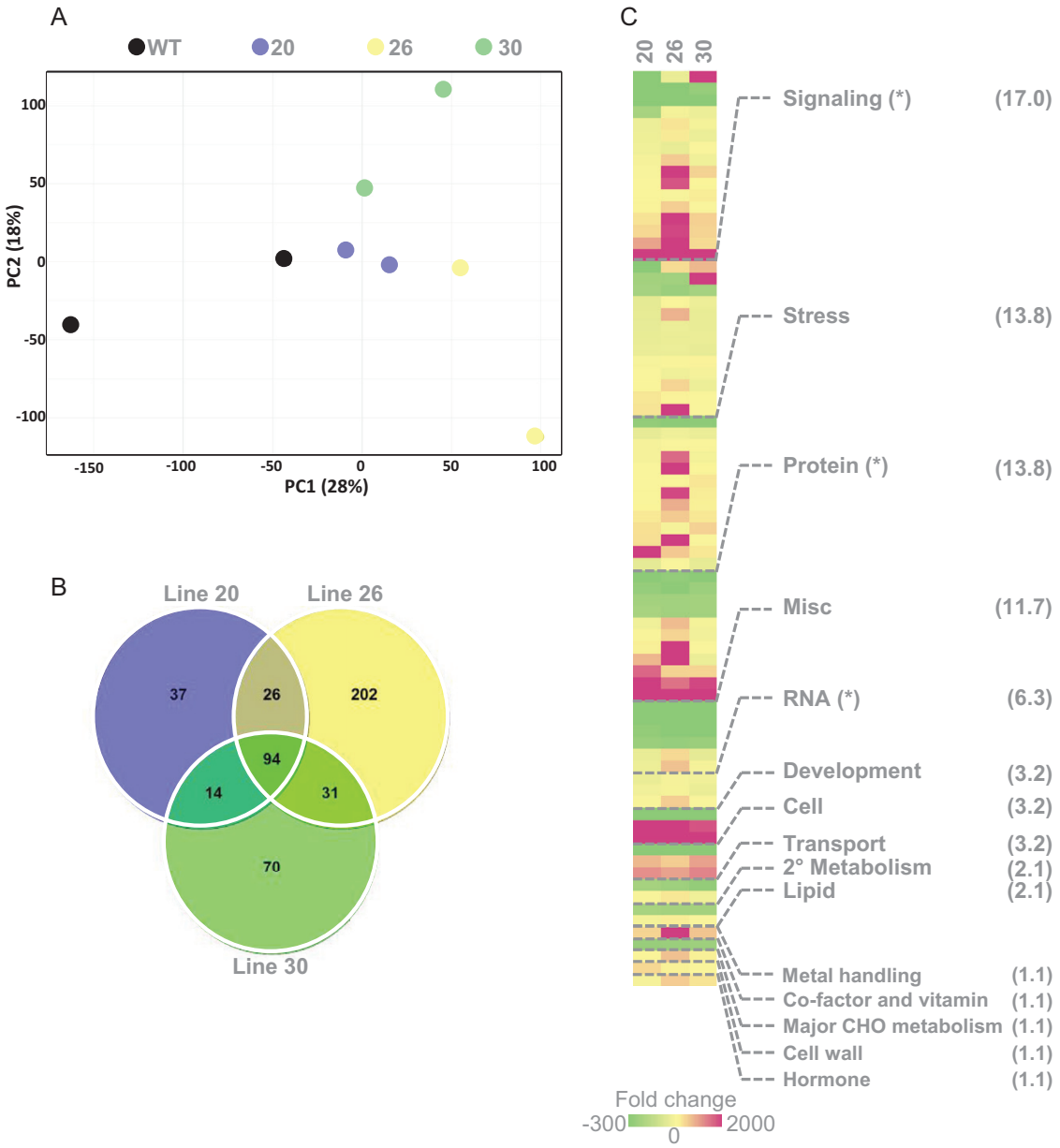

Fig. 5. Transcriptome analyses in source leaves from *NI6* silenced plants. (A) Principal component analysis (PCA) of the whole RNA-seq data set in leaves of the *NI6* silenced plants. (B) Venn diagram showing differentially expressed genes in the *NI6*-silenced lines. (C) Expression (as $\log_2$ fold changes relative to wild type controls) of the DEGs in the *NI6* silenced lines distributed onto Mapman categories. Numbers in brackets represent percentages of genes within each functional category. * denote statistically significant differences over represented categories (contingency analysis test; $P<0.01$).

Albacete *et al.*, 2014; Liu *et al.*, 2016; Shen *et al.*, 2019), results presented here extend these findings to include the role exerted by A/N-INV and their relationship with A-INV. The increase in leaf Suc content verified in the time course experiment with *NI6*-silenced plants potentially explains the transcriptional induction of *A-INV LIN6* (Solyc10g083290; Supplementary Tables S5 and S6). The up-regulation of this apoplastic invertase is associated with increases in Glc and Fru, and it has been demonstrated that LIN6 restricts carbon export from tomato (Kocal *et al.*, 2008) and tobacco (Balibrea Lara *et al.*, 2004) source leaves, altering the sink-source transition in the leaf, promoting sink metabolism in this organ (also reflected in the observed increase in hexoses). Thus, besides the effect of *NI6* silencing directly on sugar depletion in flowers (Table 2), our data exposed a further deleterious effect mediated by the up-regulation of *LIN6* (Supplementary Table S5), resulting in blockage of sugar export from source organs. This has also been recently observed in cassava plants (Yan *et al.*, 2019). In accordance with this hypothesis, expression of *SlSWEET1*, which belongs to clade I of the SWEET

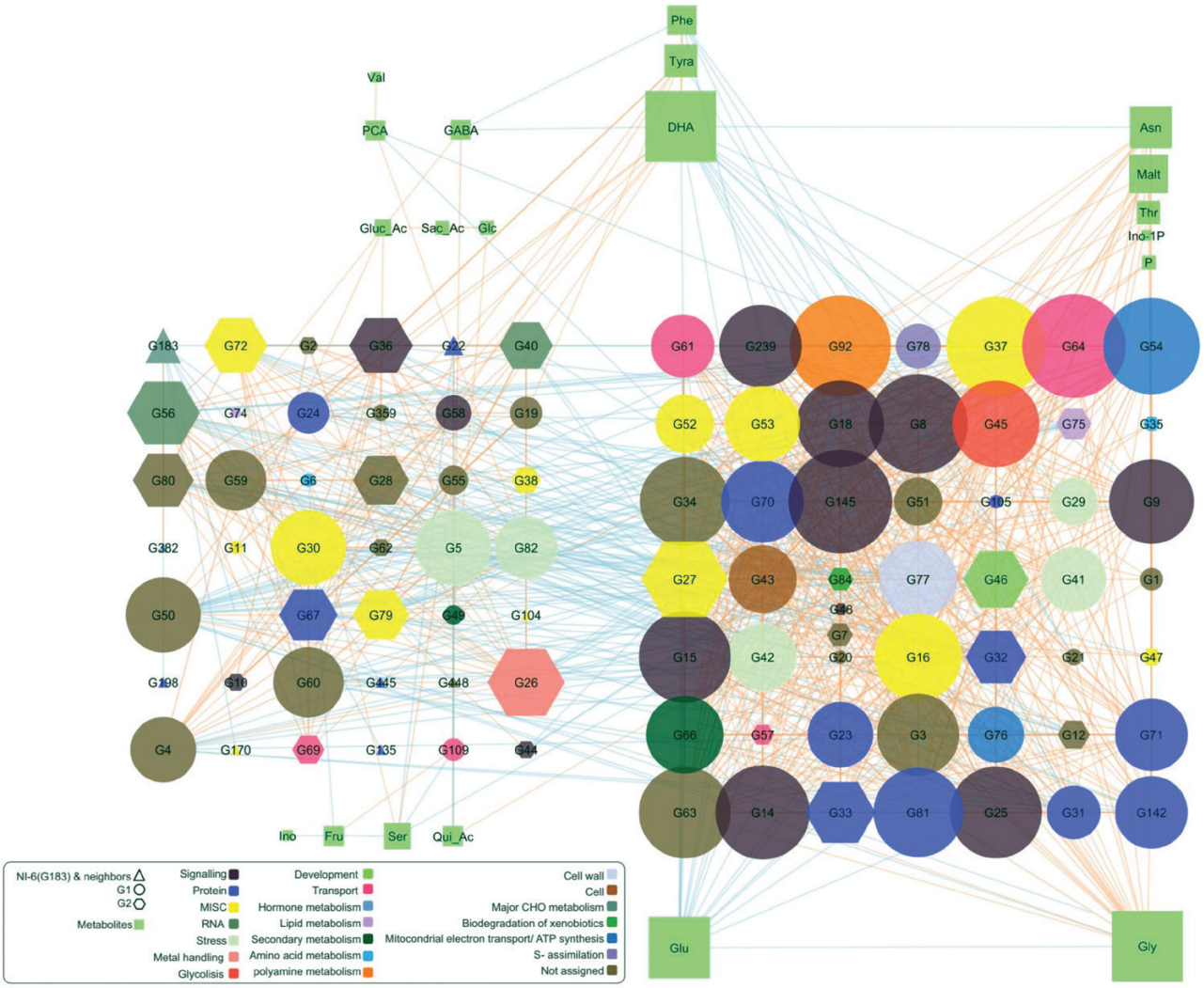

Fig. 6. Metabolite-gene network derived from canonical correlation analysis in source leaves from *NI6* silenced plants. The network comprises 20 metabolites and 92 DEGs profiled from leaves of four-week old plants. Regression values higher than |0.84| were used to infer the relevant network. Blue and red lines connect edges according to their positive or negative correlation, respectively. Circled edges correspond to loci ID as detailed in Table S6 and metabolites, respectively. Glc: glucose, Fru: fructose, Ino: inositol, SacAc: saccharic acid, Thr: threonine, P: phosphate, Phe: phenylalanine, GABA: gamma amino butyric acid, Tyra: tyramine, DHA: dehydroascorbate, Asn: asparagine.

transporter family (Ho *et al.*, 2019) is reduced. In addition, expression of *SlSUT1* (the main sucrose importer into the phloem; Hackel *et al.*, 2005) and *SlSTP2* and *SlPMT4* (two monosaccharide transporters mainly expressed in sink organs; Reuscher *et al.*, 2014) are increased (Supplementary Fig. S3).

Changes in leaf starch content are in line with reductions in the AGPase activity. However, surveying RNA-seq data revealed that expression of AGPase-encoding genes were essentially unaltered in the transformants. This observation suggests that the change in AGPase activity in these transgenic lines appears to be mediated at the post-translational level. This could be via a redox-dependent mechanism that may be activated in response to the variation of sugar content observed in the leaves of these plants, as described earlier for Arabidopsis and other plant species (Hendriks *et al.*, 2003).

In this scenario, the fact that the few fruits produced by the knock-down lines are slightly smaller can be explained by at least two mechanisms; (i) the carbon export blockage discussed above, and (ii) the elevated carbon flux control exerted by NI6 activity at the beginning and the end of fruit growth (Beauvoit *et al.*, 2014).

However, any other fruit-associated phenotype found in *NI6* knock-down plants (i.e. increases in Brix and dramatic alterations observed in their metabolite profiles) is a consequence of the tremendous effect on fruit set and harvest index, rather than a direct effect of *NI6* silencing (Colombié *et al.*, 2017).

In addition to the above-described effect of *NI6* knock-down on primary metabolism, both the metabolic and transcript profiles in vegetative tissues prior to the effect on flowering revealed that these plants exhibited alterations in the signaling

and stress systems (e.g. glutathione *S*-transferases G30, G293, G294, G350, G353, G354, and G355; superoxide dismutase G124; peroxidases G11, G47, and G169; and ATPases G194, G240, G256, and G384). One such gene which is connected to *NI6* in the reconstructed network showed consistent reduction in all three transgenic lines, and is that encoding the α-chain of the vacuolar V-type ATP synthase (G240). This vacuolar pump is essential for plant growth due to its role in energizing secondary transport, maintenance of solute homeostasis and facilitating vesicle fusion (Dietz *et al.*, 2001). A reduced expression of this vacuolar pump is in accordance with the growth reduction exhibited by the *NI6* silenced lines.

Similarly, in line with previous work, genes encoding a Kelch-like protein (G28; Solyc01g080620, Supplementary Table S6) and an inositol 1,4,5-trisphosphate 5-phosphatase (G308; Solyc08g007080) were found to be down- and up-regulated, respectively, in the leaves of *NI6* knock-down plants. Intriguingly, Sulpice *et al.* (2009) identified a Kelch-domain protein and a *myo*-inositol-1-phosphate synthase (an enzyme closely related to inositol 1,4,5-trisphosphate 5-phosphatase in inositol phosphate metabolism), whose transcripts positively and negatively correlate, respectively, with biomass accumulation in Arabidopsis plants. In view of this, one can speculate that these two genes are players in the signaling cascade affecting plant growth regulation mediated by NI6.

Several pieces of evidence indicate that A/N-INVs are required for maintaining the homeostasis of sugars and reactive oxygen species (ROS; Xiang *et al.*, 2011; Braun *et al.*, 2014). Mechanistically, an Arabidopsis A/N-INV enzyme (AT1G35580) was shown to be regulated at the post-translational level through protein phosphorylation by calcium-dependent kinases 3 and 21 (Gao *et al.*, 2014). In line with this, transcriptional profiles of *NI6* knock-down plants showed a high number of receptor-like kinase-encoding genes with altered expression pattern in the transgenic lines and enrichment in other signaling-associated genes, suggesting that *NI6* deficiency triggers a wide signaling response.

When inspecting the transcript-metabolite correlation network, it was evident that in *NI6* silenced plants there are many more genes (G1) correlating with metabolites than with changes in the expression of other genes (G2). This observation may suggest that the gene expression changes detected in the leaves of the transgenic plants are a consequence of the NI6-associated metabolic changes rather than a direct effect of NI6 as a gene expression regulator. However, considering that most of the genes in G1 belong to the signaling function category, one may speculate that the shifts observed in the growth pattern of the *NI6*-silenced plants are a consequence of a signaling cascade modulated by changes in glutamate, glycine and dehydroascorbate (DHA); the three major network hubs.

In agreement with the results presented here, the absence of A/N-INV has been previously associated with higher oxidative stress defense gene expression in Arabidopsis, while transient overexpression of *At-A/N-InvA* and *At-A/N-InvG* in leaf mesophyll protoplasts down-regulated the oxidative stress-responsive *ASCORBATE PEROXIDASE 2* (*APX2*) promoter (Xiang *et al.*, 2011). Tomato plants overexpressing the extracellular A-INV resulted in a similar effect on peroxidases (Albacete *et al.*, 2015). The leaves of *NI6* silenced plants displayed a dramatic reduction in the concentration of DHA. This observation can be understood as a consequence of the transcriptional inhibition of *APX2* promoter by a higher glucose accumulation, as discussed above (Xiang *et al.*, 2011). Along with this reduction in DHA, the leaves of *NI6* knock-down plants showed increments in the endogenous content of GABA. The central role of the GABA shunt in carbon partitioning has been emphasized (Fait *et al.*, 2008; 2011), and more recently Li *et al.* (2016) reported that the application of exogenous GABA induced heat stress tolerance in *Agrostis stolonifera,* regulating antioxidant enzyme activities and decreasing DHA content. It is then likely that the accumulation of Glu leads to the dramatic increase of GABA observed in the transgenic plants and consequently the down-regulation of DHA. Intriguingly, DHA content in ripe fruits were significantly increased either due to the decreased Glc having an opposing effect on APX2, or alternatively, indicating the existence of a regulatory mechanism of DHA homeostasis in this organ distinct from that acting in leaves in response to NI6 deficiency. In agreement with this, the silencing of monodehydroascorbate reductase in tomato had an unexpected effect on ascorbate concentration, suggesting a still unknown mechanism regulating the amounts of this compound (Gest *et al.*, 2013).

Interestingly, our results show DHA as the major hub of the gene-metabolite correlation network that split into two gene clusters, and that it is connected to Glc by only five genes, suggesting that the role of NI6 in connecting sucrose metabolism with stress response mechanisms could be mediated solely by a few genes. Among them, there is a BTB/POZ domain Kelch protein (G28; Solyc01g080620). There is not much known about the role of these proteins in plants, except for the above-mentioned observation published by Sulpice *et al.* (2009). They are described as transcriptional regulators that act through the control of chromatin structure, and as such it is reasonable to assume that it could play a regulatory role within the sugar-redox circuitry.

It is already known that sucrose is an inducer of alkaloid formation in other Solanaceae species such as *Atropa belladonna* (Rothe *et al.*, 2001; Rothe and Dräger, 2002) and potato (Richter *et al.*, 2007), and this regulation occurs at the level of expression of genes encoding biosynthetic enzymes. Our gene-metabolite network analysis suggests that this regulation may also be operating in tomato plants.

In conclusion, these results highlight the important role played by NI6, a type A/N-INV, controlling vegetative growth, carbohydrate partitioning, flowering and fruit set in tomato. *NI6* silenced lines showed dramatic alterations in these phenotypes, which were associated with changes in DEGs for stress

responses and signaling. Although convincing evidence on the role of INV in the modulation of yield in crop species of high agronomic importance, such as maize (Li *et al.*, 2013) and rice (Wang *et al.*, 2008), has been reported (reviewed by Rossi *et al.*, 2015), they focus on the importance of the apoplastic pathway for assimilate unloading, involving particularly the cell wall A-INV. Here, we presented results pointing to the importance of A/N-INV as a target for signaling pathways that coordinate carbohydrate metabolism with growth and development. Specifically, its role in sink activity is supported by (i) its high expression in sink organs such as flowers and fruits, (ii) its silencing resulting in dramatic flower abortion and reduced fruit set, and (iii) its silencing resulting in altered source-sink relationships. Analyses of transgenic plants with fruit-specific promoters should dissect the direct/indirect effects of *NI6* silencing in tomato.

Supplementary data

The following supplementary data are available at *JXB* online.

Fig. S1. Schematic representation of the NI6-GFP fusion construct.

Fig. S2. Expression of different gibberellin metabolism genes significantly altered in *NI6* knock-down lines (20, 26 and 30).

Fig. S3. Expression of different sugar transporter genes significantly altered in *NI6* knock-down lines (20, 26 and 30).

Table S1. Invertase encoding loci identified in *Solanum lycopersicum* and *Arabidopsis thaliana*.

Table S2. MIQE form, qPCR and sample information.

Table S3. Metabolite profiles of *NI6* silenced plants.

Table S4. Gene-metabolite correlation analyses.

Table S5. List of down- and up-regulated genes in source leaves of the three transgenic lines relative to wild type controls.

Table S6. Differentially expressed genes in leaves from at least one *NI6* silenced line.

Table S7. *NI6* expression measured by qPCR in different tissues from wild type tomato plants ('M82') grown under greenhouse conditions.

Table S8. Effect of *NI6* silencing on photosynthetic parameters in tomato plants.

Table S9. List of genes and RPKM values detected in leaves from four week-old plants by RNA-seq.

Acknowledgements

This work was partially supported by grants from INTA and ANPCyT (Argentina), FAPESP and CNPq (Brazil), Fondecyt 11160899 (Chile), MINECO and University of Malaga (Spain) by the Max Planck Society (Germany) and the European Union Horizon 2020 Research and Innovation Programme (Grant Agreement Number 679796). BSL and GG were recipients of fellowships from FAPESP, MR from CNPq and SO was granted by the Ramon and Cajal program (RYC-09170).

Author contributions

CCL, MC, LB, GG, IB, RA, LK, SO and FC conducted experiments; CCL, TdP, LB and EB performed RNA-seq experiments and analysed data; CCL, EB, SO, LB, MR and FC analysed data and wrote the manuscript; MG, ARF, MR, SO and FC conceived the investigation. All authors discussed the results and commented on the manuscript.

Data availability

All high-throughput sequencing data (RNA-seq) reported in this paper have been uploaded to the Sequence Read Archive (SRA) under the accession number SUB8177243.

References

Albacete A, Cantero-Navarro E, Balibrea ME, Großkinsky DK, de la Cruz González M, Martínez-Andújar C, Smigocki AC, Roitsch T, Pérez-Alfocea F. 2014. Hormonal and metabolic regulation of tomato fruit sink activity and yield under salinity. Journal of Experimental Botany **65**, 6081–6095.

Albacete A, Cantero-Navarro E, Großkinsky DK, Arias CL, Balibrea ME, Bru R, Fragner L, Ghanem ME, González MdlC, Hernández JA, *et al*. 2015. Ectopic overexpression of the cell wall invertase gene CIN1 leads to dehydration avoidance in tomato. Journal of Experimental Botany **66**, 863–878.

Balibrea Lara ME, Gonzalez Garcia M-C, Fatima T, Ehneß R, Kyun Lee T, Proels R, Tanner W, Roitsch T. 2004. Extracellular invertase is an essential component of cytokinin-mediated delay of senescence. The Plant Cell **16**, 1276–1287.

Balibrea ME, Cuartero J, Bolarín MC, Pérez-Alfocea F. 2003. Sucrolytic activities during fruit development of *Lycopersicon* genotypes differing in tolerance to salinity. Physiologia Plantarum **118**, 38–46.

Balibrea ME, Martínez-Andújar C, Cuartero J, Bolarín MC, Pérez-Alfocea F. 2006. The high fruit soluble sugar content in wild Lycopersicon species and their hybrids with cultivars depends on sucrose import during ripening rather than on sucrose metabolism. Functional Plant Biology **33**, 279–288.

Barratt DH, Derbyshire P, Findlay K, Pike M, Wellner N, Lunn J, Feil R, Simpson C, Maule AJ, Smith AM. 2009. Normal growth of Arabidopsis requires cytosolic invertase but not sucrose synthase. Proceedings of the National Academy of Sciences, USA **106**, 13124–13129.

Baxter CJ, Carrari F, Bauke A, Overy S, Hill SA, Quick PW, Fernie AR, Sweetlove LJ. 2005. Fruit carbohydrate metabolism in an introgression line of tomato with increased fruit soluble solids. Plant and Cell Physiology **46**, 425–437.

Beauvoit BP, Colombié S, Monier A, *et al.* 2014. Model-assisted analysis of sugar metabolism throughout tomato fruit development reveals enzyme and carrier properties in relation to vacuole expansion. The Plant Cell **26**, 3224–3242.

Boyer JS, McLaughlin JE. 2007. Functional reversion to identify controlling genes in multigenic responses: analysis of floral abortion. Journal of Experimental Botany **58**, 267–277.

Bradford MM. 1976. A rapid and sensitive method for the quantitation of microgram quantities of protein utilizing the principle of protein-dye binding. Analytical Biochemistry **72**, 248–254.

Braun HP, Binder S, Brennicke A, *et al.* 2014. The life of plant mitochondrial complex I. Mitochondrion **19 Pt B**, 295–313.

Carrari F, Fernie AR. 2006. Metabolic regulation underlying tomato fruit development. Journal of Experimental Botany **57**, 1883–1897.

Colombié S, Beauvoit B, Nazaret C, *et al.* 2017. Respiration climacteric in tomato fruits elucidated by constraint-based modelling. New Phytologist **213**, 1726–1739.

De Godoy F, Bermúdez L, Lira BS, *et al.* 2013. Galacturonosyltransferase 4 silencing alters pectin composition and carbon partitioning in tomato. Journal of Experimental Botany **64**, 2449–2466.

Di Rienzo JA, Casanoves F, Balzarini M, Gonzalez L, Tablada M, Robledo C. 2016. Infostat. Sofware estadístico. Argentina: Universidad Nacional de Córdoba. http://www.infostat.com.ar/

Dietz KJ, Tavakoli N, Kluge C, Mimura T, Sharma SS, Harris GC, Chardonnens AN, Golldack D. 2001. Significance of the V-type ATPase for the adaptation to stressful growth conditions and its regulation on the molecular and biochemical level. Journal of Experimental Botany **52**, 1969–1980.

Fait A, Fromm H, Walter D, Galili G, Fernie AR. 2008. Highway or byway: the metabolic role of the GABA shunt in plants. Trends in Plant Science **13**, 14–19.

Fait A, Nesi AN, Angelovici R, Lehmann M, Pham PA, Song L, Haslam RP, Napier JA, Galili G, Fernie AR. 2011. Targeted enhancement of glutamate-to-γ-aminobutyrate conversion in Arabidopsis seeds affects carbon-nitrogen balance and storage reserves in a development-dependent manner. Plant Physiology **157**, 1026–1042.

Fridman E, Carrari F, Liu YS, Fernie AR, Zamir D. 2004. Zooming in on a quantitative trait for tomato yield using interspecific introgressions. Science **305**, 1786–1789.

Gao J, van Kleeff PJ, Oecking C, Li KW, Erban A, Kopka J, Hincha DK, de Boer AH. 2014. Light modulated activity of root alkaline/neutral invertase involves the interaction with 14-3-3 proteins. The Plant Journal **80**, 785–796.

Gest N, Garchery C, Gautier H, Jiménez A, Stevens R. 2013. Light-dependent regulation of ascorbate in tomato by a monodehydroascorbate reductase localized in peroxisomes and the cytosol. Plant Biotechnology Journal **11**, 344–354.

Gibon Y, Bläsing OE, Palacios-Rojas N, Pankovic D, Hendriks JH, Fisahn J, Höhne M, Günther M, Stitt M. 2004. Adjustment of diurnal starch turnover to short days: depletion of sugar during the night leads to a temporary inhibition of carbohydrate utilization, accumulation of sugars and post-translational activation of ADP-glucose pyrophosphorylase in the following light period. The Plant Journal **39**, 847–862.

Goetz M, Roitsch T. 1999. The different pH optima and substrate specificities of extracellular and vacuolar invertases from plants are determined by a single amino-acid substitution. The Plant Journal **20**, 707–711.

Goff LA, Trapnell C, Kelley D. 2012. cummeRbund: analysis, exploration, manipulation, and visualization of Cufflinks high-throughput sequencing data R Package Version 2.2.

Goodstein DM, Shu S, Howson R, *et al.* 2012. Phytozome: a comparative platform for green plant genomics. Nucleic Acids Research **40**, D1178–D1186.

Hackel A, Schauer N, Carrari F, Fernie AR, Grimm B, Kühn C. 2006. Sucrose transporter LeSUT1 and LeSUT2 inhibition affects tomato fruit development in different ways. The Plant Journal **45**, 180–192.

Hendriks JH, Kolbe A, Gibon Y, Stitt M, Geigenberger P. 2003. ADP-glucose pyrophosphorylase is activated by posttranslational redox-modification in response to light and to sugars in leaves of Arabidopsis and other plant species. Plant Physiology **133**, 838–849.

Ho L-H, Klemens PAW, Neuhaus HE, Ko H-Y, Hsieh S-Y, Guo W-J. 2019. SlSWEET1a is involved in glucose import to young leaves in tomato plants. Journal of Experimental Botany **70**, 3241–3254.

Jang JC, León P, Zhou L, Sheen J. 1997. Hexokinase as a sugar sensor in higher plants. The Plant Cell **9**, 5–19.

Jia L, Zhang B, Mao C, Li J, Wu Y, Wu P, Wu Z. 2008. OsCYT-INV1 for alkaline/neutral invertase is involved in root cell development and reproductivity in rice (*Oryza sativa* L.). Planta **228**, 51–59.

Jin Y, Ni DA, Ruan YL. 2009. Post-translational elevation of cell wall invertase activity by silencing its inhibitor in tomato delays leaf senescence and increases seed weight and fruit hexose level. The Plant Cell **21**, 2072–2089.

Kamenetzky L, Asís R, Bassi S, *et al.* 2010. Genomic analysis of wild tomato introgressions determining metabolism- and yield-associated traits. Plant Physiology **152**, 1772–1786.

Karimi M, Inzé D, Depicker A. 2002. GATEWAYTM vectors for Agrobacterium-mediated plant transformation. Trends in Plant Science, 193–195. doi: 10.1016/S1360-1385(02)02251-3.

Kocal N, Sonnewald U, Sonnewald S. 2008. Cell wall-bound invertase limits sucrose export and is involved in symptom development and inhibition of photosynthesis during compatible interaction between tomato and *Xanthomonas campestris* pv *vesicatoria*. Plant Physiology **148**, 1523–1536.

Kühn C, Barker L, Bürkle L, Frommer W. 1999. Update on sucrose transport in higher plants. Journal of Experimental Botany **50**, 935–953.

Lammens W, Le Roy K, Schroeven L, Van Laere A, Rabijns A, Van den Ende W. 2009. Structural insights into glycoside hydrolase family 32 and 68 enzymes: functional implications. Journal of Experimental Botany **60**, 727–740.

Langmead B, Salzberg SL. 2012. Fast gapped-read alignment with Bowtie 2. Nature Methods **9**, 357–359.

Li B, Liu H, Zhang Y, Kang T, Zhang L, Tong J, Xiao L, Zhang H. 2013. Constitutive expression of cell wall invertase genes increases grain yield and starch content in maize. Plant Biotechnology Journal **11**, 1080–1091.

Li Z, Palmer WM, Martin AP, Wang R, Rainsford F, Jin Y, Patrick JW, Yang Y, Ruan YL. 2012. High invertase activity in tomato reproductive organs correlates with enhanced sucrose import into, and heat tolerance of, young fruit. Journal of Experimental Botany **63**, 1155–1166.

Li Z, Yu J, Peng Y, Huang B. 2016. Metabolic pathways regulated by abscisic acid, salicylic acid and γ-aminobutyric acid in association with improved drought tolerance in creeping bentgrass (*Agrostis stolonifera*) Physiologia Plantarum. Nature Publishing Group, (June), 1–16. doi: 10.1111/ppl.12483.

Liu YH, Offler CE, Ruan YL. 2016. Cell wall invertase promotes fruit set under heat stress by suppressing ROS-independent cell death. Plant Physiology **172**, 163–180.

Lohse M, Nagel A, Herter T, May P, Schroda M, Zrenner R, Tohge T, Fernie AR, Stitt M, Usadel B. 2014. Mercator: a fast and simple web server for genome scale functional annotation of plant sequence data. Plant Cell and Environment **37**, 1250–1258.

Luedemann A, Strassburg K, Erban A, Kopka J. 2008. TagFinder for the quantitative analysis of gas chromatography-mass spectrometry (GC-MS)-based metabolite profiling experiments. Bioinformatics **24**, 732–737.

Martín ML, Lechner L, Zabaleta EJ, Salerno GL. 2013. A mitochondrial alkaline/neutral invertase isoform (A/N-InvC) functions in developmental energy-demanding processes in Arabidopsis. Planta **237**, 813–822.

Meng LS, Wei ZQ, Cao XY, Tong C, Lv MJ, Yu F, Loake GJ. 2020. Cytosolic invertase-mediated root growth is feedback regulated by a glucose-dependent signaling loop. Plant Physiology **184**, 895–908.

Murayama S, Handa H. 2007. Genes for alkaline/neutral invertase in rice: alkaline/neutral invertases are located in plant mitochondria and also in plastids. Planta **225**, 1193–1203.

Nahirñak V, Almasia NI, Fernandez PV, Hopp HE, Estevez JM, Carrari F, Vazquez-Rovere C. 2012. Potato Snakin-1 gene silencing affects cell division, primary metabolism, and cell wall composition. Plant Physiology **158**, 252-263.

Notredame C, Higgins DG, Heringa J. 2000. T-Coffee: a novel method for fast and accurate multiple sequence alignment. Journal of Molecular Biology **302**, 205–217.

Nunes-Nesi A, Araújo WL, Fernie AR. 2011. Targeting mitochondrial metabolism and machinery as a means to enhance photosynthesis. Plant Physiology **155**, 101–107.

Nunes-Nesi A, Carrari F, Lytovchenko A, Smith AM, Loureiro ME, Ratcliffe RG, Sweetlove LJ, Fernie AR. 2005. Enhanced photosynthetic performance and growth as a consequence of decreasing mitochondrial malate dehydrogenase activity in transgenic tomato plants. Plant Physiology **137**, 611–622.

Pan L, Guo Q, Chai S, *et al*. 2019. Evolutionary conservation and expression patterns of neutral/alkaline invertases in Solanum. Biomolecules. **9**(12). doi: 10.3390/biom9120763

Prudent M, Lecomte A, Bouchet JP, Bertin N, Causse M, Genard M. 2011. Combining ecophysiological modelling and quantitative trait locus analysis to identify key elementary processes underlying tomato fruit sugar concentration. Journal of Experimental Botany **62**, 907–919.

Qi X, Wu Z, Li J, Mo X, Wu S, Chu J, Wu P. 2007. AtCYT-INV1, a neutral invertase, is involved in osmotic stress-induced inhibition on lateral root growth in Arabidopsis. Plant Molecular Biology **64**, 575–587.

Qin G, Zhu Z, Wang W, Cai J, Chen Y, Li L, Tian S. 2016. A tomato vacuolar invertase inhibitor mediates sucrose metabolism and influences fruit ripening. Plant Physiology **172**, 1596–1611.

Ramakers C, Ruijter JM, Deprez RH, Moorman AF. 2003. Assumption-free analysis of quantitative real-time polymerase chain reaction (PCR) data. Neuroscience Letters **339**, 62–66.

R Development Core Team. 2015. R: A language and environment for statistical computing. R Foundation for Statistical Computing, Vienna.

Reuscher D, Akiyama M, Yasuda R, Makino H, Aoki K, Shibata D, Shiratake K. 2014. The sugar transporter inventory of tomato: genome-wide identification and expression analysis. Plant and Cell Physiology **55**, 1123–1141.

Richter U, Sonnewald U, Dräger B. 2007. Calystegines in potatoes with genetically engineered carbohydrate metabolism. Journal of Experimental Botany **58**, 1603–1615.

Roessner-Tunali U, Liu J, Leisse A, Balbo I, Perez-Melis A, Willmitzer L, Fernie AR. 2004. Kinetics of labelling of organic and amino acids in potato tubers by gas chromatography-mass spectrometry following incubation in (13)C labelled isotopes. The Plant Journal **39**, 668–679.

Rolland F, Moore B, Sheen J. 2002. Sugar sensing and signaling in plants. The Plant Cell **14 Suppl**, S185–S205.

Rossi M, Bermudez L, Carrari F. 2015. Crop yield: challenges from a metabolic perspective. Current Opinion in Plant Biology **25**, 79–89.

Rothe G, Dräger B. 2002. Tropane alkaloids. Metabolic response to carbohydrate signal in root cultures of Atropa belladonna. Plant Science **163**, 979–985.

Rothe G, Garske U, Dräger B. 2001. Calystegines in root cultures of *Atropa belladonna* respond to sucrose, not to elicitation. Plant Science **160**, 1043–1053.

Sauvage C, Segura V, Bauchet G, Stevens R, Do PT, Nikoloski Z, Fernie AR, Causse M. 2014. Genome-wide association in tomato reveals 44 candidate loci for fruit metabolic traits. Plant Physiology **165**, 1120–1132.

Shannon P, Markiel A, Ozier O, Baliga NS, Wang JT, Ramage D, Amin N, Schwikowski B, Ideker T. 2003. Cytoscape: a software environment for integrated models of biomolecular interaction networks. Genome Research **13**, 2498–2504.

Shen S, Ma S, Liu Y, Liao S, Li J, Wu L, Kartika D, Mock HP, Ruan YL. 2019. Cell wall invertase and sugar transporters are differentially activated in tomato styles and ovaries during pollination and fertilization. Frontiers in Plant Science **10**, 506.

Sonnewald U, Hajirezaei MR, Kossmann J, Heyer A, Trethewey RN, Willmitzer L. 1997. Increased potato tuber size resulting from apoplastic expression of a yeast invertase. Nature Biotechnology **15**, 794–797.

Stitt M, Lilley RMcC, Gerhardt R, Heldt HW. 1989. Metabolite levels in specific cells and sub-cellular compartments of plant leaves. Methods in Enzymology **174**, 518–552.

Sturm A. 1999. Invertases. Primary structures, functions, and roles in plant development and sucrose partitioning. Plant Physiology **121**, 1–8.

Sturm A, Tang GQ. 1999. The sucrose-cleaving enzymes of plants are crucial for development, growth and carbon partitioning. Trends in Plant Science **4**, 401–407.

Sulpice R, Pyl ET, Ishihara H, *et al.* 2009. Starch as a major integrator in the regulation of plant growth. Proceedings of the National Academy of Sciences, USA **106**, 10348–10353.

Szarka A, Horemans N, Passarella S, Tarcsay A, Orsi F, Salgó A, Bánhegyi G. 2008. Demonstration of an intramitochondrial invertase activity and the corresponding sugar transporters of the inner mitochondrial membrane in Jerusalem artichoke (*Helianthus tuberosus* L.) tubers. Planta **228**, 765–775.

Tamoi M, Tabuchi T, Demuratani M, Otori K, Tanabe N, Maruta T, Shigeoka S. 2010. Point mutation of a plastidic invertase inhibits development of the photosynthetic apparatus and enhances nitrate assimilation in sugar-treated Arabidopsis seedlings. The Journal of Biological Chemistry **285**, 15399–15407.

Tamura K, Stecher G, Peterson D, Filipski A, Kumar S. 2013. MEGA6: molecular evolutionary genetics analysis version 6.0. Molecular Biology and Evolution **30**, 2725–2729.

Tiessen A, Hendriks JHM, Stitt M, Branscheid A, Gibon Y, Farré EM, Geigenberger P. 2002. Starch synthesis in potato tubers is regulated by post-translational redox modification of ADP-glucose pyrophosphorylase. American Society of Plant Biologists 2191–2213. doi: 10.1105/tpc.003640.2192.

Tiessen A, Prescha K, Branscheid A, Palacios N, McKibbin R, Halford NG, Geigenberger P. 2003. Evidence that SNF1-related kinase and hexokinase are involved in separate sugar-signalling pathways modulating post-translational redox activation of ADP-glucose pyrophosphorylase in potato tubers. The Plant Journal **35**, 490–500.

Trapnell C, Pachter L, Salzberg SL. 2009. TopHat: discovering splice junctions with RNA-Seq. Bioinformatics **25**, 1105–1111.

Trapnell C, Roberts A, Goff L, Pertea G, Kim D, Kelley DR, Pimentel H, Salzberg SL, Rinn JL, Pachter L. 2012. Differential gene and transcript expression analysis of RNA-seq experiments with TopHat and Cufflinks. Nature Protocols **7**, 562–578.

Tymowska-Lalanne Z, Kreis M. 1998. Expression of the *Arabidopsis thaliana* invertase gene family. Planta **207**, 259–265.

Urbanczyk-Wochniak E, Usadel B, Thimm O, *et al.* 2006. Conversion of MapMan to allow the analysis of transcript data from Solanaceous species: effects of genetic and environmental alterations in energy metabolism in the leaf. Plant Molecular Biology **60**, 773–792.

Vargas W, Cumino A, Salerno GL. 2003. Cyanobacterial alkaline/neutral invertases. Origin of sucrose hydrolysis in the plant cytosol? Planta **216**, 951–960.

Vargas WA, Pontis HG, Salerno GL. 2007. Differential expression of alkaline and neutral invertases in response to environmental stresses: characterization of an alkaline isoform as a stress-response enzyme in wheat leaves. Planta **226**, 1535–1545.

Vargas WA, Pontis HG, Salerno GL. 2008. New insights on sucrose metabolism: evidence for an active A/N-Inv in chloroplasts uncovers a novel component of the intracellular carbon trafficking. Planta **227**, 795–807.

Walker RP, Winters AL, Pollock CJ. 1997. Purification and characterization of invertases from leaves of *Lolium temulentum*. New Phytologist **135**, 259–266.

Wan N, DeLorenzo DM, He L, *et al.* 2017. Cyanobacterial carbon metabolism: fluxome plasticity and oxygen dependence. Biotechnology and Bioengineering **114**, 1593–1602.

Wan H, Wu L, Yang Y, Zhou G, Ruan YL. 2018. Evolution of sucrose metabolism: the dichotomy of invertases and beyond. Trends in Plant Science **23**, 163–177.

Wang YQ, Wei XL, Xu HL, *et al.* 2008. Cell-wall invertases from rice are differentially expressed in Caryopsis during the grain filling stage. Journal of Integrative Plant Biology **50**, 466–474.

Ward JM, Kühn C, Tegeder M, Frommer WB. 1998. Update on sucrose transport in higher plants. Journal of Experimental Botany **178**, 41–71.

Welham T, Pike J, Horst I, *et al.* 2009. A cytosolic invertase is required for normal growth and cell development in the model legume, Lotus japonicus. Journal of Experimental Botany **60**, 3353–3365.

Wilson AM, Work TM, Bushway AA, Bushway RJ. 1981. HPLC determination of fructose, glucose, and sucrose in potatoes. Journal of Food Science **46**, 300–301.

Xiang L, Le Roy K, Bolouri-Moghaddam MR, Vanhaecke M, Lammens W, Rolland F, Van den Ende W. 2011. Exploring the neutral invertase-oxidative stress defence connection in *Arabidopsis thaliana*. Journal of Experimental Botany **62**, 3849–3862.

Xie J, Cai K, Hu HX, Jiang YL, Yang F, Hu PF, Cao DD, Li WF, Chen Y, Zhou CZ. 2016. Structural analysis of the catalytic mechanism and substrate specificity of anabaena alkaline invertase InvA reveals a novel glucosidase. The Journal of Biological Chemistry **291**, 25667–25677.

Yan W, Wu X, Li Y, Liu G, Cui Z, Jiang T, Ma Q, Luo L, Zhang P. 2019. Cell wall invertase 3 affects cassava productivity via regulating sugar allocation from source to sink. Frontiers in Plant Science **10**, 541.

Yao SG, Kodama R, Wang H, Ichii M, Taketa S, Yoshida H. 2009. Analysis of the rice SHORT-ROOT5 gene revealed functional diversification of plant neutral/alkaline invertase family. Plant Science **176**, 627–634.

Zanor MI, Osorio S, Nunes-Nesi A, *et al.* 2009. RNA interference of LIN5 in tomato confirms its role in controlling Brix content, uncovers the influence of sugars on the levels of fruit hormones, and demonstrates the importance of sucrose cleavage for normal fruit development and fertility. Plant Physiology **150**, 1204–1218.

Zrenner R, Salanoubat M, Willmitzer L, Sonnewald U. 1995. Evidence of the crucial role of sucrose synthase for sink strength using transgenic potato plants (Solanum tuberosum L.). The Plant Journal 97–107. doi: 10.1046/j.1365-313X.1995.07010097.x.